Contents

List of Figures

List of Tables

Glossary

RNA-Seq	Transcriptome data from sequencing RNA.
synthetic lethal	Genetic interactions where inactivation of multiple genes is inviable (or deleterious) which are viable if inactivated separately.

Acronyms

ANOVA	Analysis of Variance.
AUROC	Area under the receiver operating characteristic (curve).
BiSEp	Bimodal Subsetting Expression.
DNA	Deoxyribonucleic acid.
HPC	High Performance Computing.
mtSLIPT	Synthetic Lethal Interaction Prediction Tool (with respect to mutation).
NeSI	New Zealand eScience Infrastructure.
PI3K	Phosphoinositide 3-kinase.
ROC	Reciever operating characteristic (curve).
siRNA	Short interfering ribonucleic acid.
SLIPT	Synthetic lethal interaction prediction tool.
Slurm	Simple Linux Utility for Resource Management.
TCGA	The Cancer Genome Atlas (genomics project).

Chapter 6

Simulation and Modeling of Synthetic Lethal Pathways

Simulation and modelling of synthetic lethality in gene expression is revisited in greater detail in this chapter, building upon the results which supported the use of SLIPT (in Section 3.3) . In Chapter 3, a simulation procedure for generating simulated data with underlying (known) synthetic lethal partners of a query gene, such as *CDH1*, was developed (as described in Section 3.2.2) by sampling from a Multivariate normal distribution based on a statistical model of synthetic lethality in expression data (as described in Section 3.2.1). This simulation framework was applied to simulated data (in Section 3.3), including simple correlation structures to assess the statistical performance of the SLIPT methodology and support its use as a computational approach for detecting synthetic lethal candidates from expression data throughout this thesis (Chapters 4 and 5).

While this basic framework was provided some support for the use of SLIPT, further investigations with simulations were conducted to assess the strengths and limitations of the SLIPT methodology, compare it to alternative statistical approaches to synthetic lethal detection, and assess its performance under more complex correlation structures. Together these simulation investigations assess the performance of the SLIPT methodology, including on pathway graph structures (e.g., those discussed in Chapter 5) and indicate whether the SLIPT methodology (or similar refined bioinformatics strategies) are statistically rigourous or suitable for wider genomics applications.

These simulation investigations continue to utilise the Multivariate Normal simulation procedure (as applied in Section 3.3) with further refinements. The SLIPT methodology (and the χ^2 test) were applied across a range of parameters (including

altering the quantiles for detecting synthetic lethal direction and compared to correlation). This was also applied to query correlated genes (as performed in Section 3.3).

A refined simulation procedure was developed specifically to extend the methodology described in Section 3.2 to utilise pathway graph structures for the correlation structures of simulated datasets (as described in Section 3.4.2). This methodology can be applied to simulated correlation structures across simple graph structures to test specific network modules or use pathway structures based on biological pathways. Thus graph structure and simulation approaches were combined to test whether a gene locus in a pathway affects detection by SLIPT and whether SLIPT performance is affected by pathway structure. The simulation procedure based on graph structures was applied in a computational pipeline across many parameter combinations using high-performance computing resources (as discussed in Section 2.5.3) and the core simulation functions have been released as a software package for wider use to test bioinformatics and statistical methods on graph structures (as described in Section 3.5.3).

6.1 Synthetic Lethal Detection Methods

The SLIPT methodology (as it has been applied throughout Chapters 4 and 5) was compared for alternative computational approaches to detecting synthetic lethality in simulated gene expression data. As discussed in Section 3.3, this procedure enables testing ability of SLIPT to detect known synthetic lethal partner genes by sampling from a statistical model of synthetic lethality. While comprehensive benchmarking has not been performed, several approaches to synthetic lethal detection are considered (e.g., Pearson correlation, the χ^2 test, and testing for bimodality) to evaluate the strengths of the SLIPT methodology, including modifications to the parameters of SLIPT.

The following comparisons of simulations of computational detection of synthetic lethality with different statistical rationales suffice to discuss the strengths of SLIPT, evaluate whether it is appropriate for further application in genomics research, and identify limitations which may be addressed with further developments. Some potential avenues for further development of computational synthetic lethal discovery will be discussed in Section 7.3.

6.1.1 Performance of SLIPT and χ^2 across Quantiles

Simulated datasets with synthetic lethal partner genes were generated using the multivariate normal simulation procedure (as described in Section 3.2.2) with performance

assessed using area under the receiver operating characteristic (AUROC) analysis (as described in Section 2.3.5). Synthetic lethal detection was compared for modifications to the SLIPT methodology (as described in Section 3.1), namely that the quantiles used to define low and high expression was varied. Rather, than $1/3$ (as used throughout this thesis) the samples below the lowest $1/n$ quantile and above the highest $1/n$ quantile were used for SLIPT (and the χ^2-test) to detect lowly and highly expressing samples respectively. The quantiles tested range from 2, splitting at the $1/2$ quantile (the median), to 100, using the lowest (1%) and highest (99%) percentiles.

This enables testing of the threshold for lowly expressing genes which is most able to distinguish synthetic lethal genes, even with higher-order synthetic lethal interactions (as discussed in Section 3.2.1). Both SLIPT with the directional criteria for synthetic lethality and significance of the equivalent χ^2 test were performed for each quantile. Pearson correlation was also tested on simulated continuous expression data for synthetic lethal detection in simulated data, considering both positive and negative correlations separately as predictors of synthetic lethality for comparison with χ^2 based approaches, using discete categories fo gene function deriving from quantiles.

The results presented throughout this section use the example of 5 synthetic lethal partners to illustrate the differences in performance between the standard SLIPT procedure (slipt-3) to n quantiles (slipt-n), the χ^2-test on the same quantiles, and positive or negative correlation. However, similar results across different numbers of known synthetic lethal genes are shown in Appendix J. The synthetic lethal detection procedures were compared with 10,000 simulations of a small dataset of 100 genes and 1000 samples without correlation structure between genes, as performed in Section 3.3.2) . As shown in Figure 6.1, the 3-quantiles previously used have optimal performance and SLIPT has a comparable or higher performance than the χ^2-test alone across quantiles.

Pearson correlation was also tested as a predictor of synthetic lethality (i.e., whether highly positive or negative correlations with the query gene detected synthetic lethal partners). Positive correlation performed worse than random (with an AUROC lower than 0.5) as thus coexpression of genes is not predictive of synthetic lethality in simulated data. Conversely, negative correlation is predictive of synthetic lethality, consistent with synthetic lethal gene activity being mutually exclusive. However, neither correlation approach performed as well as the optimal quantiles for the SLIPT procedure or χ^2-test.

These results are shown in both a bargraph and lineplot to show the individual results of each parameter, and to compare SLIPT with the χ^2-test side-by-side across

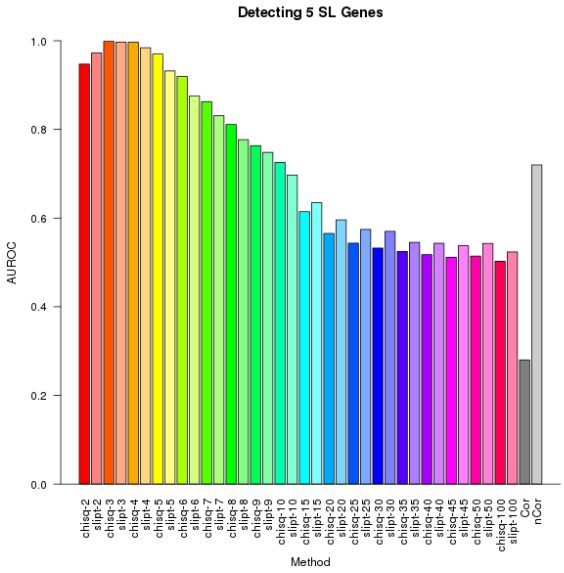

(a) Barplot of χ^2, SLIPT, and correlation.

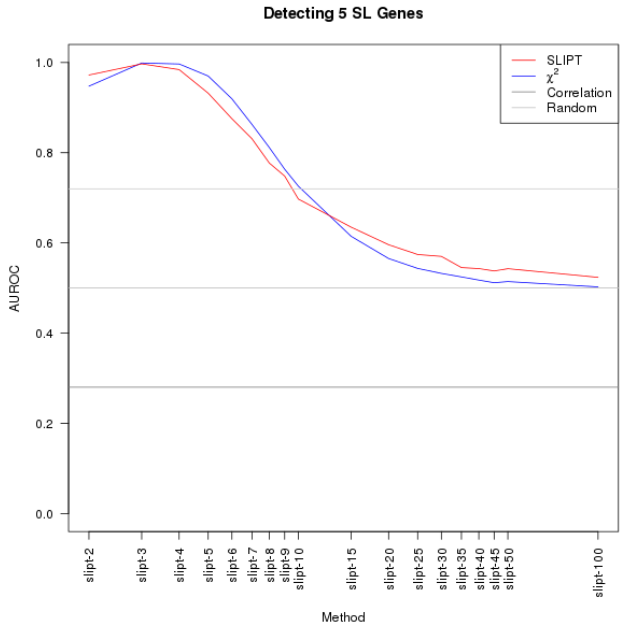

(b) Lineplot of χ^2, SLIPT, and correlation.

Figure 6.1: **Performance of χ^2 and SLIPT across quantiles**. Synthetic lethal detection (of 5 genes) with quantiles as on the axes. The barplot uses the same hues for each quantile (grey for correlation) and darker for χ^2 (and positive correlation). The line plot (with log-scale quantiles) is coloured according to the legend. SLIPT and χ^2 perform similarly, peaking at $^1/_3$-quantiles and converging to random (0.5). Negative correlation was higher than positive but not optimal quantiles for SLIPT or χ^2.

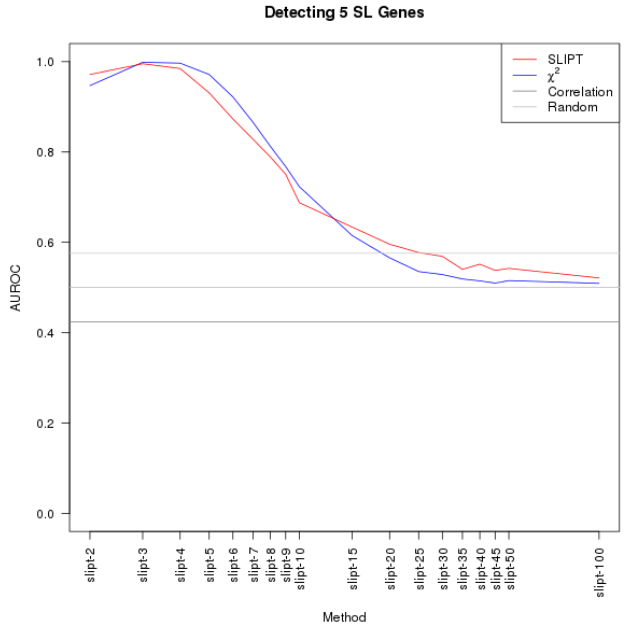

Figure 6.2: **Performance of χ^2 and SLIPT across quantiles with more genes**. Synthetic lethal detection (of 5 genes in 20,000) with quantiles as in axis labels. The line plot (with log-scale quantiles) is coloured according to the legend. As for simulations with fewer genes, SLIPT and χ^2 perform similarly, peaking at $^1/_3$-quantiles and converging to random (0.5). Negative correlation was higher than positive but not optimal quantiles for SLIPT or χ^2.

quantiles. Similarly, these plots are given for detecting a range of known synthetic lethal partners in the simulations in Figures J.1 and J.2. These demonstrate that the findings shown for 5 synthetic lethal genes are robust across different numbers of underlying synthetic lethal genes.

The synthetic lethal detection procedures were also tested with 1000 simulations of a larger dataset of 20,000 genes and 1000 samples. While fewer simulations gives a less accurate receiver operating characteristic (ROC) result, this is sufficient to replicate the above findings with a feasible number of genes in a human gene expression dataset and assess the impact of a higher proportion of non synthetic lethal genes (potential false positives). Simulated datasets of this size were also used in Section 3.3.2 to test the specificity in a number of genes similar to that in experimental datasets for cancer genomes. As shown in Figure 6.2, the above findings were replicated in simulations of a larger dataset with 20,000 genes. These were also robustly replicated across varying numbers of underlying synthetic lethal genes (as shown in Figure J.3).

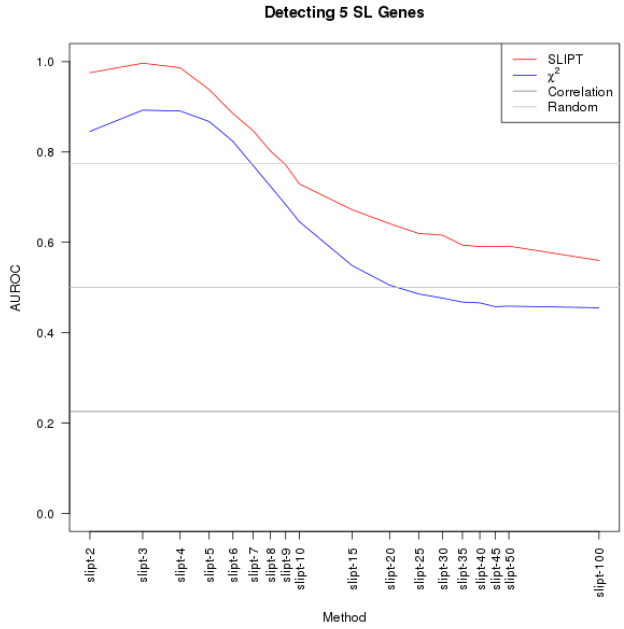

Figure 6.3: **Performance of χ^2 and SLIPT across quantiles with query correlation**. Synthetic lethal detection (of 5 genes in 100 including 5 query correlated) with quantiles as in axis labels. The line plot (with log-scale quantiles) is coloured according to the legend. SLIPT performs consistently higher than χ^2 due to higher specificity. Negative correlation performed modestly.

6.1.1.1 Correlated Query Genes affects Specificity

As discussed in Section 3.3.2.2, positively correlated genes (with the query gene) have an impact of on the performance of synthetic lethal detection. SLIPT was able to distinguish these from synthetic lethal partners and hence is likely to have a higher specificity in datasets which include positively correlated genes with the query gene (as expected in gene expression data). The synthetic lethal detection procedures were compared with 10,000 simulations of a small dataset of 100 genes (with 5 correlated with the query gene) and 1000 samples otherwise without correlation structure between genes. As shown in Figure 6.3, this specificity is reflected in the increased AUROC performance values for SLIPT (in contrast to Figure 6.1). This specificity can be attributed to the directional criteria (as described in Section 3.1) since the χ^2-test alone performs comparatively poorly with positively correlated genes.

The synthetic lethal detection procedures were also compared with 1000 simulations of a larger dataset of 20,000 genes (with 1000 correlated with the query gene) and 1000 samples otherwise without correlation structure between genes. This simulation

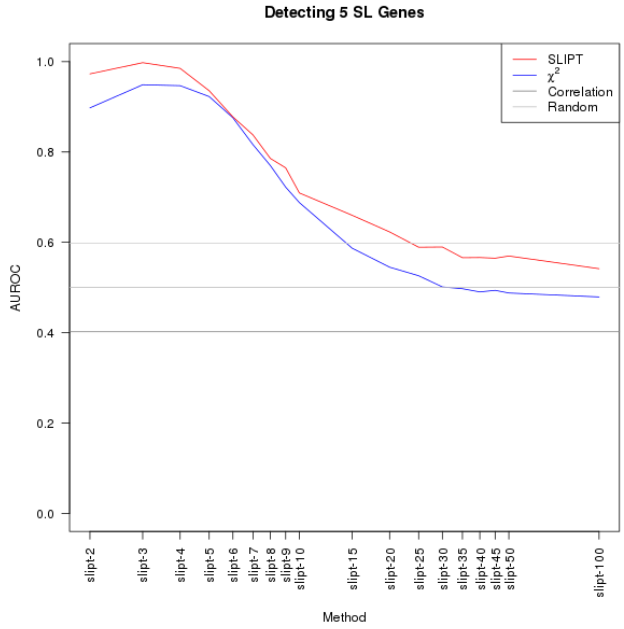

Figure 6.4: **Performance of χ^2 and SLIPT across quantiles with query correlation and more genes**. Synthetic lethal detection (of 5 genes in 20,000 including 1000 query correlated) with quantiles as in axis labels. The line plot (with log-scale quantiles) is coloured according to the legend. SLIPT performs consistently higher than χ^2 due to higher specificity. Negative correlation performed modestly.

increases the number of genes (and proportion of negative genes) to those comparable with a human gene expression dataset while maintaining a comparable 5% of positively correlated genes. As shown in Figure 6.4, SLIPT still outperforms χ^2 or negative correlation and is optimal at the 3-quantile. The difference between SLIPT and χ^2 was less pronounced in a larger dataset with many weakly correlated genes. The greater specificity of SLIPT than χ^2-test to distinguish positively correlated non synthetic lethal genes is not as evident with a large number of negative genes (as potential false positives). However, specificity is an important consideration in large-scale genomics analysis where there are potentially many false positives.

Nevertheless, SLIPT with 3-quantiles (as performed throughout Chapters 4 and 5), had higher performance than when other quantile thresholds were used, particularly when positive correlations were present (replicating the Section 3.3.2.2). These findings hold across different numbers of underlying synthetic lethal genes (as shown in Figures J.5 and J.6).

Together these results support the use of SLIPT, particularly the use of quantiles as thresholds for gene function and specific use of 3-quantiles which perform well compared to other quantiles. A particular concern in the design of SLIPT for expression data whether the samples sizes are sufficient when the data is divided into quantiles. The SLIPT methodology further performed better for 3-quantiles (and other moderate values) than χ^2 or correlation as a predictor of synthetic lethality. These results are irrespective of sample size or p-value threshold since the results replicated across sample sizes and the AUROC values were independent significance thresholds. Using a moderate number of quantiles for SLIPT ensures that there are a sufficient number of samples expected below and above them so that deviations from these are statistically detectable. These quantiles were also optimal for the χ^2 test which uses the same expected values asthe SLIPT directional conditions.

6.1.2 Alternative Synthetic Lethal Detection Strategies

The SLIPT approach (and χ^2) to detect synthetic lethality from binning expression to estimate gene function also outperforms correlations which use continuous data directly. Correlation performing poorly as a synthetic lethal detection strategy consistent with there not necessarily being a relationship between synthetic lethal partners which can be in distinct biological pathways, expressed at different times or in different cell types. Nevertheless, correlation is among the alternative detection methods considered in further detail.

The BImodal Subsetting ExPression (BiSEp) R package (Wappett, 2014) for using bimodality to detect synthetic lethality (Wappett *et al.*, 2016) were also considered, along with a linear regression approach. These statistical methods span a range of computational approaches to detecting synthetic lethality and serve to compare alternatives to SLIPT, supporting its design and application. However, these comparisons are able provide supporting data from statistical modelling and simulations for the viability of the SLIPT methodology for synthetic lethal discovery in cancer (as demonstrated in Chapter 4) and further applications.

6.1.2.1 Correlation for Synthetic Lethal Detection

As shown in Section 6.1.1, negative (Pearson) correlation performed better than positive correlation, indicating the inverse relationships were more predictive of synthetic lethality. However, neither correlation approach performed as well as SLIPT or the χ^2 test as a predictor of synthetic lethal gene partners. It is notable that negative correlation still often performed considerably better than random chance.

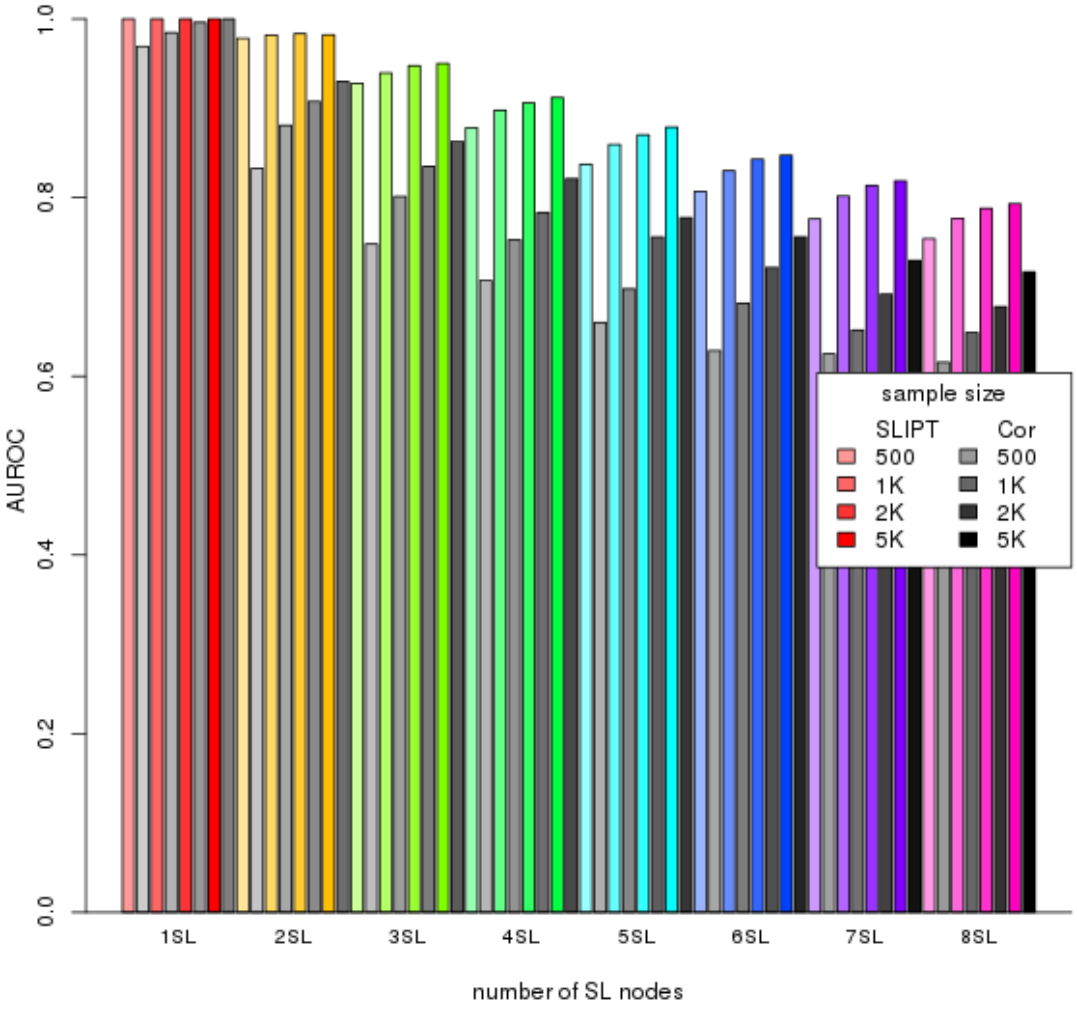

Figure 6.5: **Performance of negative correlation and SLIPT**. Synthetic lethal detection with SLIPT was compared to negative (Pearson) correlation across parameters. SLIPT consistently outperformed correlation. Both approaches had lower performance for more synthetic lethal partners and lower sample sizes. 10,000 simulations were performed with correlation structure as used in Section 6.2.1.2

Negative correlation was compared directly to the SLIPT methodology (as described in Section 3.1) across numbers of known synthetic lethal partners and sample size (ranging from 500 to 5000). This comparison used 1000 simulations of a dataset with 20,000 genes and synthetic lethal genes from within a network (sampled as in Section 3.4.2)) with a 0.8 correlation between adjacent genes. In a direct comparison of

SLIPT and negative correlation (shown in Figure 6.5), SLIPT consistently has higher performance in simulated data across parameter values and (inverse) correlation-based approaches perform modestly in comparison. Thus using thresholds to categorise expression data (as performed by SLIPT and χ^2) does not compromise the performance of these methods by losing continuous data that would be used for calculating correlations. Similarly, the slope of a linear regression did not perform as well at synthetic lethal detection than SLIPT.

Both SLIPT and correlation had poorer performance with increasing numbers of the synthetic lethal genes to detect, while they had higher performance in higher sample sizes, as expected (as previously observed for SLIPT in Section 3.3). Thus the issue with detection of greater numbers of synthetic lethal genes is not specific to SLIPT but occurs across computational methods of synthetic lethal discovery in (simulated) expression data and likely stems from cryptic higher-order synthetic lethal interactions (as conservatively assumed in Section 3.2.1).

6.1.2.2 Testing for Bimodality with BiSEp

Extensive attempts were also made to compare SLIPT to the BiSEp methodology (Wappett *et al.*, 2016), a statistical approach to identify synthetic lethal gene pairs from mutually exclusive relationships using bimodal distributions. This synthetic lethal detection methodology is also designed for expression analysis in cancer and is readily available as an (open-source) R package (Wappett, 2014), a practice which facilitates adoption and testing of the methodology on the same datasets and simulations procedures as previously used for SLIPT.

The BiSEp package is designed for global testing of all potential gene pairs in the genome for synthetic lethality rather than focusing on the search space of potential partners of the query gene. This approach was unable to detect synthetic lethal gene pairs in the TCGA breast cancer expression dataset (TCGA, 2012). However, this may be due to stringent thresholds under the multiple testing of millions of potential gene pairs.

For a direct comparison with the query-based SLIPT approach, the source code of the BiSEp R functions was modified to test solely for the partners of a specific gene. This approach was still unable to detect synthetic lethal partners of *CDH1* in TCGA breast cancer expression data (TCGA, 2012), even with the detection thresholds for bimodality and significance greatly relaxed from those which the package defaults to.

To circumvent multiple testing issues, BiSEp only tests gene pairs for synthetic lethality between genes with a detectable bimodal distribution. However, even with

relaxed thresholds, bimodal distributions were not detectable in the normalised TCGA data (TCGA, 2012). Such normalisation Ritchie *et al.* (2015) is standard practice for expression datasets generated from microarrays or RNA-Seq and therefore BiSEp may not be appropriate to apply to this data. However, it is noted that BiSEp may also use other data types such as DNA copy number or cell line data for which it may be more applicable (Wappett *et al.*, 2016).

Nevertheless, attempts were made to test BiSEp on simulated datasets with underlying synthetic lethal genes (using the procedures described in Sections 3.2.2 and 3.4.2). However, BiSEp was also unable to detect genes with bimodal distributions of genes (and thus unable to detect synthetic lethality) in a limited number of computationally intensive simulations. Therefore investigations on a wider range of parameters were not performed.

6.2 Simulations with Graph Structures

Simulations of synthetic lethality in Section 3.3 included correlated blocks of genes as a rudimentary model of pathway structure and co-regulated genes. Here the simulation procedure was expanded to account for more complex graph structures by sampling from multivariate normal distributions with correlation structure derived from graph structures (as described in Section 3.4.2). This approach enables simulation of synthetic lethal pathways with known correlation structure and known partners (of a gene not in the pathway) and evaluation of the performance of SLIPT under simple controlled correlation structures and complex correlations such as those derived from biological networks (e.g., those described in Chapter 5). The SLIPT methodology will be tested both in artificial constructed networks to evaluate the effect of pathway structure on synthetic lethal detection, including large biologically feasible pathways to test whether SLIPT is robust under complex correlation structures and applicable to such complex genomics data.

These simulations combine the approach of prior simulation analyses (in Sections 3.3 and 6.1) with the graph structures for biological pathways (as used in Chapter 5). This enables testing whether subtle or large differences in pathway structure affect synthetic lethal detection, whether inhibiting relationships (or inverse correlations) between genes affect synthetic lethal detection, and whether synthetic lethal detection varies by which gene is synthetic lethal and which genes are closely linked within the pathway structure. In addition, large numbers of synthetic lethal genes and biologically feasible numbers of genes (with many non-synthetic lethal genes) will be tested to

replicate the findings of Sections 3.3 and 6.1 in correlated structures derived from pathway graphs, including examples of biological pathways from Reactome (Croft *et al.*, 2014).

Simple and more complex constructed graph structures will be used to demonstrate the impact of pathway structure of the performance of SLIPT for synthetic lethal detection in simulations. In addition, more complex constructed graph structures will be compared to the phosphoinositide 3-kinase (PI3K) and $G_{\alpha i}$ signalling pathways derived from Reactome will be used for simulation of pathway structures of biological complexity (as shown in Figures 5.1 and F.4).

6.2.1 Performance over a Graph Structure

6.2.1.1 Simple Graph Structures

Simple pathway modules were used to test the effect of pathway structure on the performance of detecting synthetic lethal partners within graph structures. To start with, the graph structures (shown by Figure 6.6) were used where a gene has one upstream regulator and two downstream (Figure 6.6b) or a gene has two upstream regulators and one downstream gene (Figure 6.6b). SLIPT has a high performance in these simulations, detecting randomly selected synthetic lethal partners in small simple networks (as shown in Figures 6.7 and K.1).

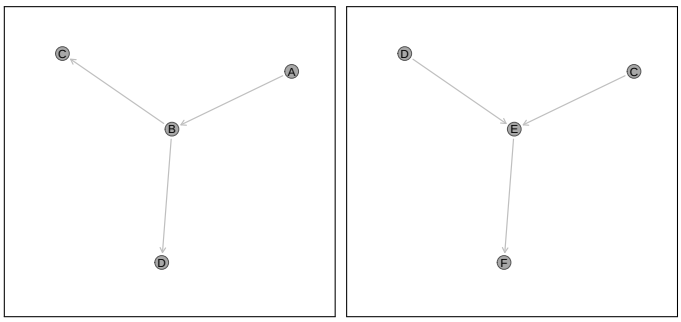

(a) Diverging Module (b) Converging Module

Figure 6.6: **Simple graph structures.** A simple graph structures used to demonstrate the simulation procedure. These are examples of a pathway diverging or converging respectively which enables testing the importance of direction in pathway structures. These are used with both activating and inhibiting relationships as shown.

As previously observed (in Section 3.3), performance declines with higher numbers of synthetic lethal genes and lower sample sizes. However, the sensitivity of SLIPT

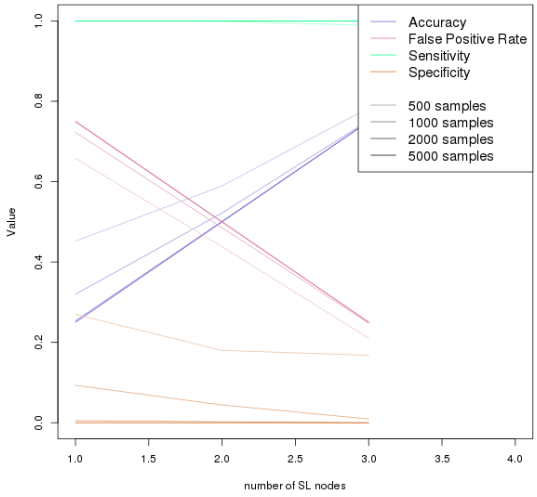

(a) Statistical evaluation

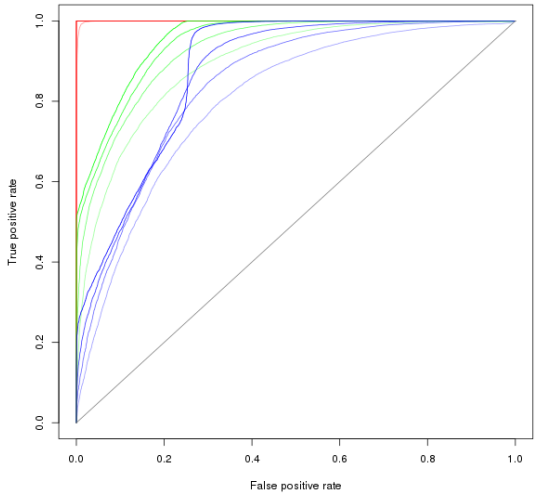

(b) Receiver operating characteristic

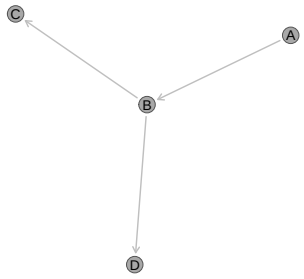

(c) Graph Structure

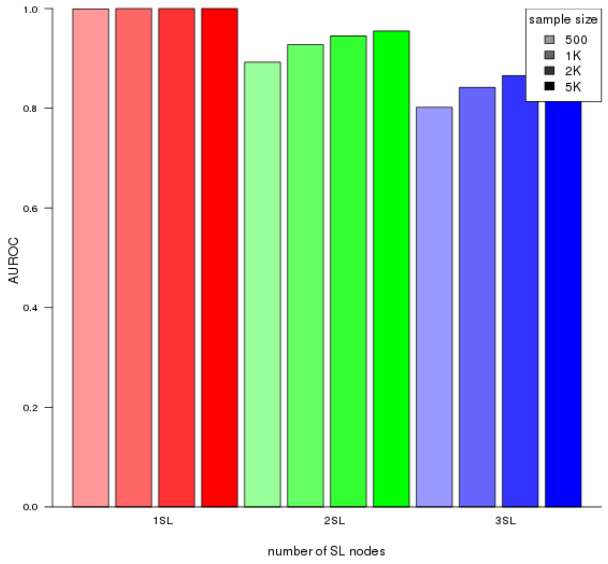

(d) Statistical performance

Figure 6.7: **Performance of simulations on a simple graph.** Simulation of synthetic lethality was performed sampling from a multivariate normal distribution generated from a diverging graph structure. Performance of SLIPT declines for more synthetic partners but this is mitigated by increased sample sizes (in darker colours). This manifests as a decline in specificity and the false positive rate. For each parameter value, 10,000 simulations were used. Colours of the ROC curves in Figure 6.7b correspond to the parameters in Figure 6.7d.

is high with conventional p-value thresholds (adjusted by {glsFDR). Thus synthetic lethal partners are often distinguishable for non synthetic lethal genes, even in simple highly correlated networks. The small number of genes and their high correlation has an impact on the ROC curves for higher numbers of synthetic lethal partners which are skewed compared to those observed previously. Note that specificity cannot be tested if all potential partner genes are synthetic lethal which limits the number of synthetic lethal genes which can be tested.

These results are particularly consistent between the pathway modules of diverging (in Figure 6.8a) and converging signals (in Figure 6.8b), with the AUROC performance and underlying curves being strikingly similar between these graph structures (as shown in Figures 6.7 and K.1). This indicates that the performance of SLIPT is not perturbed by pathway structure, in particular the direction of pathway relationships, as these graph structures also demonstrate pathways in opposite direction. In a direct comparison (shown in Figure 6.8c), the performance of simulations in these simple graphs does not differ across parameter values and therefore SLIPT is robust to pathway direction.

6.2.1.2 Constructed Graph Structures

A more complex graph structure was used to test the performance of detecting synthetic lethal partners with SLIPT in simulated expression data with pathway correlation structures. For a simple chain of gene representing a pathway (shown in Figure 6.9), the above findings were generally replicated. Performance was high across parameter values in small networks, with similar decreases in higher numbers of synthetic lethal genes to detect and lower sample size.

When detecting synthetic lethal genes with SLIPT using adjusted ({glsFDR) p-value thresholds, the performance differences can be largely attributed to changes in specificity as the small numbers of synthetic lethal genes produce highly significant p-values. Despite lower specificity and performance in ROC curves, the accuracy increases and false positive rate decreases desirably with higher numbers of synthetic lethal genes due to the high sensitivity and proportion of synthetic lethal genes detected. Therefore the thresholds imposed by adjusted p-values appear to be appropriate for detecting synthetic lethal partners, even in strongly correlated pathways, at least in these small-scale test cases.

However, an artifact of these small test cases is the skewed ROC curves (as discussed in Section 6.2.1.1) which may be related to the low number of non-synthetic lethal genes to identify as true negatives, affecting the accuracy of specificity. This is

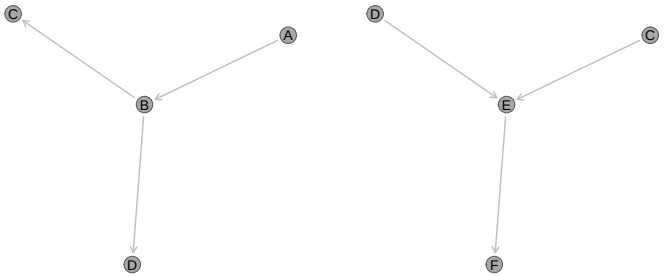

(a) Diverging Module (b) Converging Module

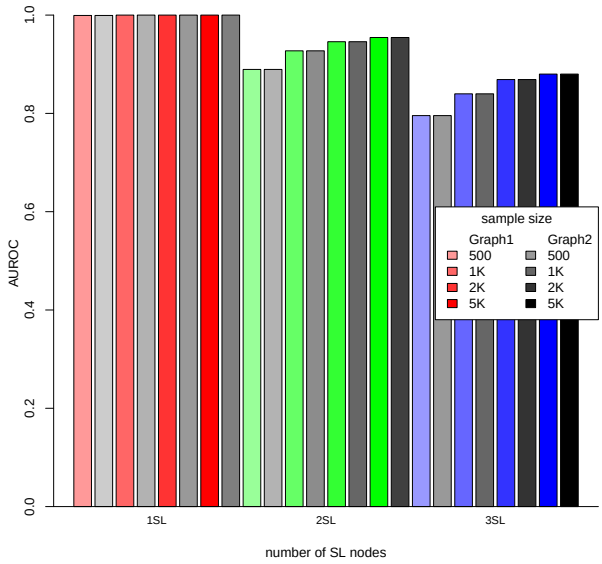

(c) Performance Between Graph Structures

Figure 6.8: **Performance of simulations is similar in simple graphs.** The AUROC values for simulations of multivariate normal distributions based on each graph structure yielded indistinguishable performance across parameter values in 10,000 simulations.

unlikely to occur in large expression datasets with many non synthetic lethal genes, as shown previously (in Section 3.3) and 6.2.1.1) in simulations of graphs structures in larger datasets (in Section 6.2.4). This does not occur in larger, more complex graphs structures, even with modest total numbers of genes and high correlations (as shown in Section 6.3).

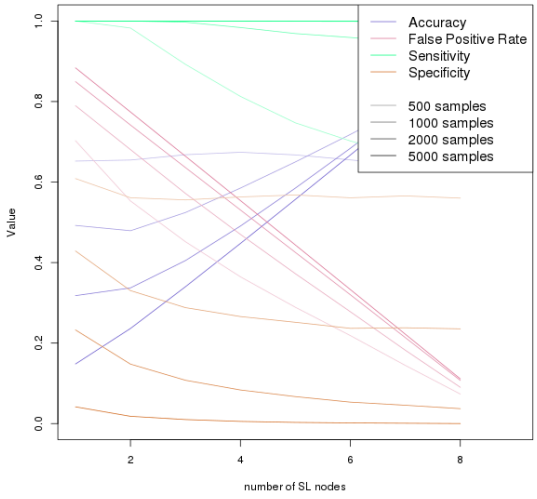

(a) Statistical evaluation

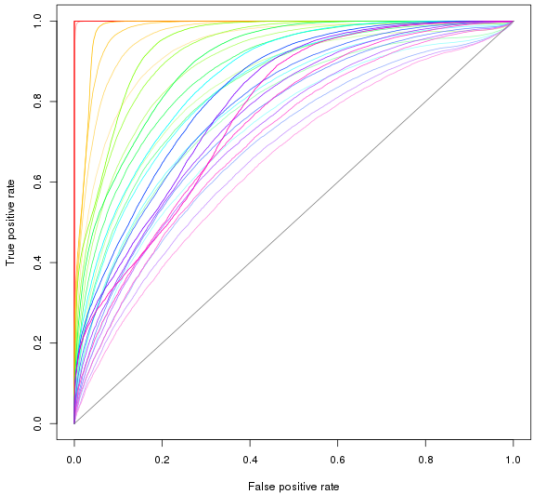

(b) Receiver operating characteristic

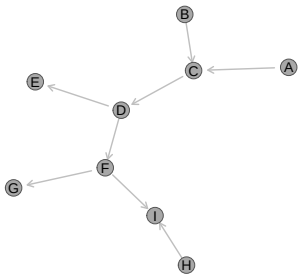

(c) Graph Structure

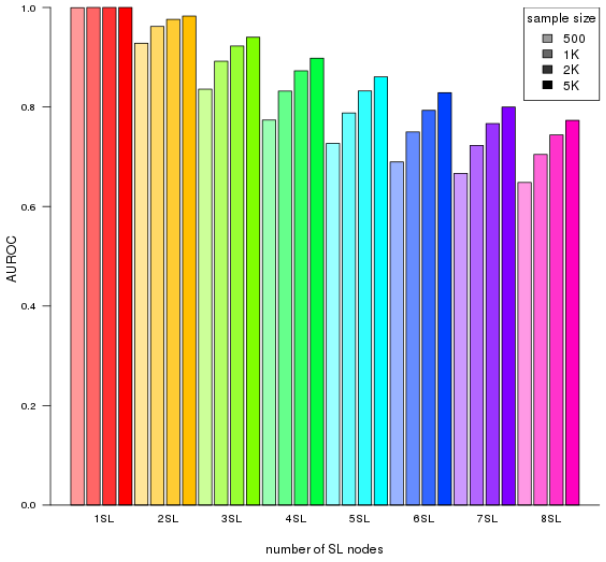

(d) Statistical performance

Figure 6.9: **Performance of simulations on a pathway.** Simulation of synthetic lethality was performed sampling from a multivariate normal distribution generated from a pathway structure. Performance of SLIPT declines for more synthetic partners and lower sample sizes (in darker colours). For each parameter value, 10,000 simulations were used. Colours of the ROC curves in Figure 6.9b correspond to the parameters in Figure 6.9d.

6.2.2 Performance with Inhibitions

Simulations of synthetic lethality in expression data were also performed with correlation structures derived from graphs containing inhibiting relationships (as are commonplace in biological pathways) which produce negative correlations. As shown in Figure 6.10, these are not an issue for detection by SLIPT. Rather, the SLIPT procedure performs well on simple graph modules with highly negative correlations. With synthetic lethal detection based on p-value (adjusted by {glsFDR), there was higher specificity, higher accuracy, and lower false positive rate in an inhibitory graph than the same graph with activating relationships (as shown by Figure 6.7).

The ROC curves for an inhibiting graph also show consistently high specificity irrespective of detection threshold with only the upper extreme of the curve exhibiting a skew below random performance (in Figure 6.10). Nevertheless, the AUROC values show a high performance across parameter values, particularly avoiding issues with higher numbers of synthetic lethal partners (as observed in Section 6.2.1.1). However, performance was marginally lower for higher numbers of synthetic lethal genes to detect and lower sample sizes, consistent with previously observations.

Negatively correlated simulated datasets are also unperturbed by minor differences in graph structure, such as changing in the direction of the graph module. As observed for activating relationships in these graph modules, the performance was highly concordant between the graph modules (shown by similar results in Figures 6.10 and K.2).

Detection of synthetic lethality by SLIPT in simulated data with inhibiting relationships outperforms simulations with activating relationships in the same graph structure (as shown in Figure 6.11). Thus SLIPT is robust in gene expression datasets with inverse correlations and performs well in them, at least in simple test cases. This is important because such relationships occur frequently in biological pathways and therefore the findings inferred from graph structures without inhibiting relationships are a conservative estimate.

The SLIPT methodology likely performs better in biological pathways (which contain negative correlations) than the graph structures discussed previously (in Section 6.2.1). This is likely since negative correlations lead to synthetic lethal partners and inversely correlated genes which are positively correlated with the query gene. As previously shown, the SLIPT methodology performs well with specificity against positively correlated query genes (in Sections 3.3.2.2 and 6.1.2.1).

Similarly, more complex graph structures with entirely inhibiting relationships (negative correlations) also perform desirably on p-value thresholds (adjusted by {glsFDR)

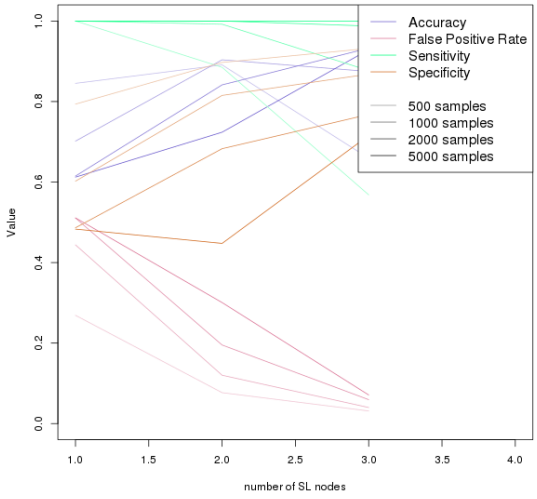

(a) Statistical evaluation

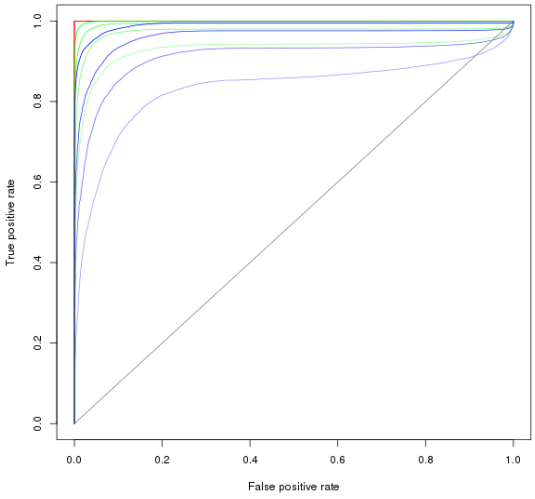

(b) Receiver operating characteristic

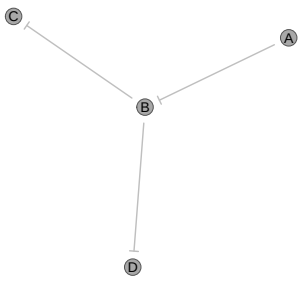

(c) Graph Structure

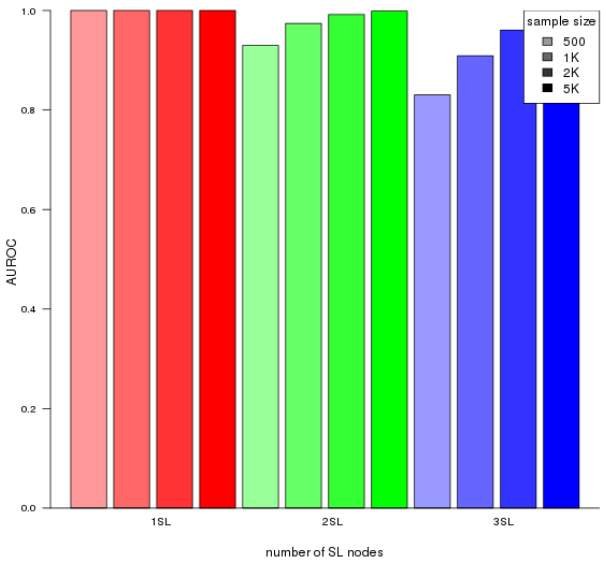

(d) Statistical performance

Figure 6.10: **Performance of simulations on a simple graph with inhibition.** Simulation of synthetic lethality was performed sampling from a multivariate normal distribution generated from an inhibiting graph. Performance of SLIPT declines for more synthetic partners and lower sample sizes. For each parameter value, 10,000 simulations were used. Colours of the ROC curves in Figure 6.10b correspond to the parameters in Figure 6.10d.

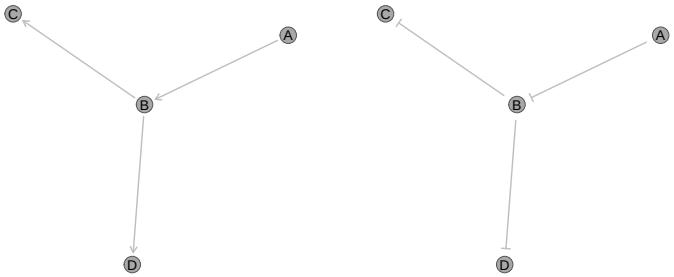

(a) Activating Graph (b) Inhibiting Graph

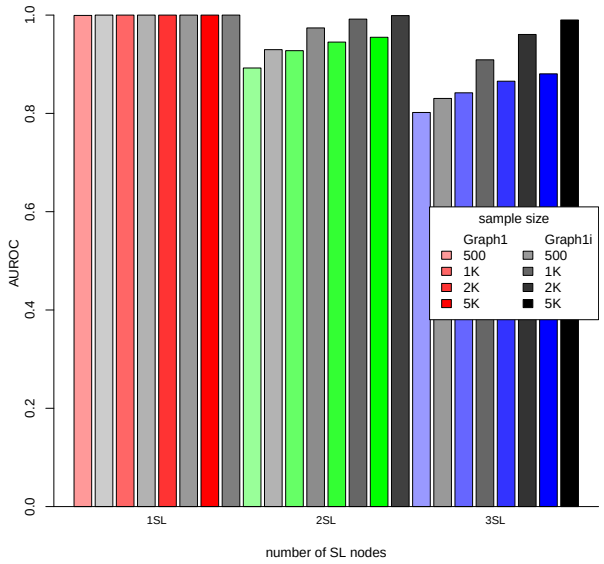

(c) Performance Between Graph Structures

Figure 6.11: **Performance is higher on a simple inhibiting graph.** The AUROC values for simulations of multivariate normal distributions based on inhibitions in the Graph structure yielded consistently higher performance across parameter values in 10,000 simulations.

and have high performance across increasing numbers of synthetic lethal genes, particularly for sufficiently high sample sizes (as shown by Figure K.3). However, this is not necessarily the case for graph structures with a combination of activating and inhibiting relationships (i.e., containing positive and negative correlations) As shown by Figure K.4, such a mixed network structure does not necessarily have high performance across parameters as observed for purely inhibiting networks.

These still appear to have desirably high sensitivity, high accuracy, and low false positive rate for detecting more synthetic lethal genes, despite poor specificity. The

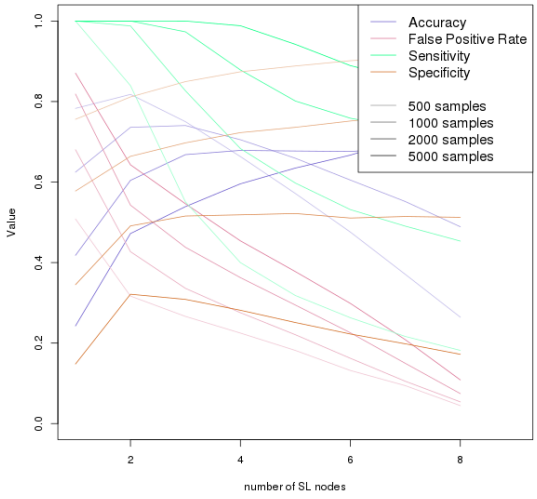

(a) Statistical evaluation

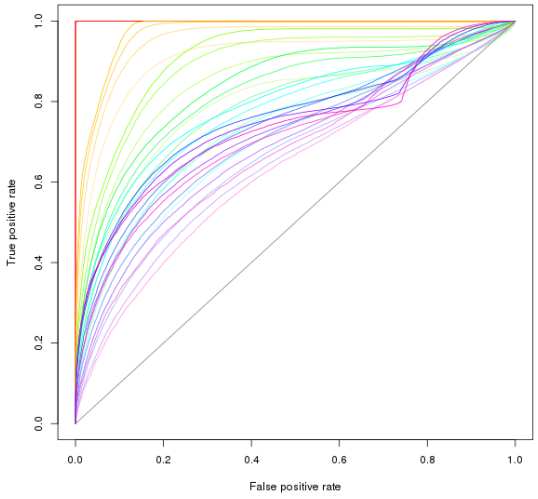

(b) Receiver operating characteristic

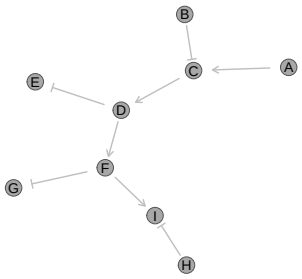

(c) Graph Structure

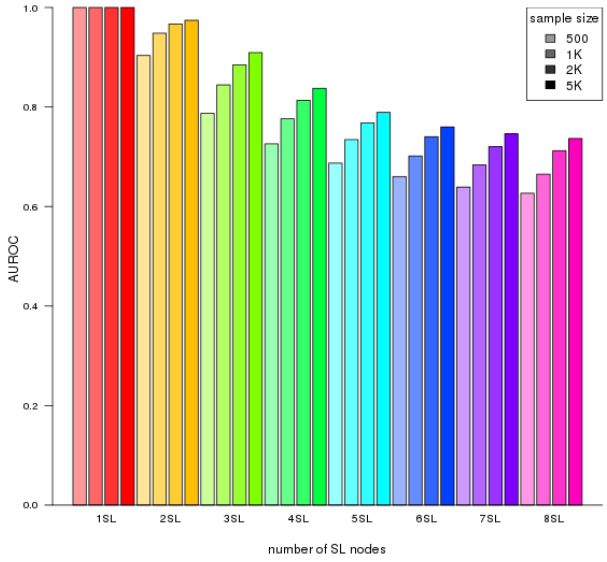

(d) Statistical performance

Figure 6.12: **Performance of simulations on a constructed graph with inhibition.** Simulation of synthetic lethality was performed sampling from a multivariate normal distribution generated from pathway structure with a combination of inhibitions. Performance of SLIPT declines for more synthetic partners and lower sample sizes. For each parameter value, 10,000 simulations were used.

ROC curves are particularly skewed for high proportions of the network being synthetic lethal and may stem from low numbers of true negative genes to detect (as discussed in Section 6.2.1.1). In a direct comparison of performance (shown in Figure 6.13), the purely inhibiting graph had consistently higher performance than the activating one as observed for simpler graphs (in Figure 6.11).

In contrast, the combination of activating and inhibiting relationships had slightly lower performance across parameters compared to the same graph structure with activating relationships. Therefore correlation structure can impact on the performance of SLIPT in a graph network, in either direction, specifically the addition of negative correlations. However, this may be an artifact of the simulation procedure as synthetic lethal genes from the correlation structure were randomly selected (without regard to their relationships), with the query gene added to ensure that conditions for synthetic lethal relationships were met.

This system for simulating inhibitory pathways is not ideal since it lead to synthetic lethal gene combinations, by randomly selecting them, which are unlikely to occur in biological pathways. These randomly selected synthetic lethal genes may account for the detection results being suboptimal (i.e., difficult to detect synthetic lethal partners) compared to previous investigations. It is expected that inversely correlated synthetic partner genes will be highly expressed in a mutually exclusive manner such that at least one of them will be compensating for loss of the query gene in most samples, leading to a weak synthetic lethal signature in expression data in this case. Furthermore, this case may not be representative of empirical biological data with synthetic lethal partners of tumour suppressor genes which are commonly inversely correlated to the query gene (to some extent) and therefore it is unlikely that they are strongly negative correlated with each other, unless they are synthetic lethal partners of each other as well. It is plausible that many synthetic lethal partner genes will serve to separately compensate for the loss of query gene function and be positively correlated with each other. Nonetheless, these simulations are sufficient to demonstrate that correlation structure (particularly negative correlations) have an impact on the detection of synthetic lethality. However, SLIPT is still able to perform well across graphs with different activating and inhibiting relationships and the perturbations in performance are marginal, particularly those reducing performance compared to an activating network.

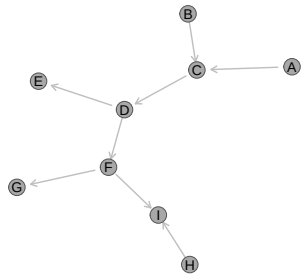

(a) Activating Graph

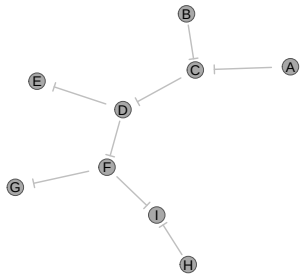

(b) Inhibiting Graph

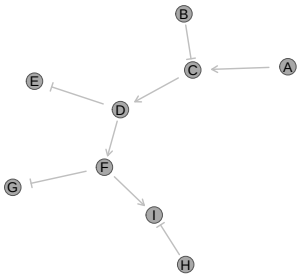

(c) Mixed Graph

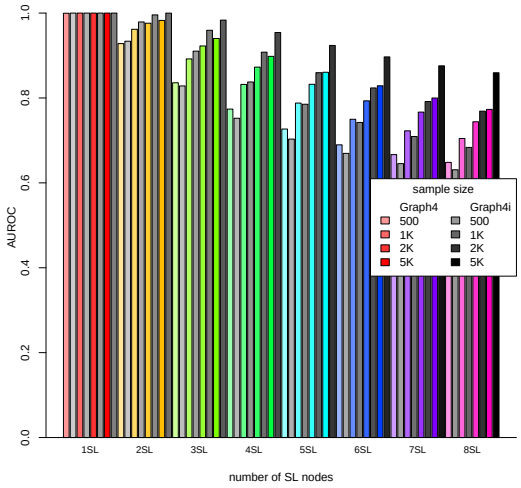

(d) Performance Between Graphs (a) and (b)

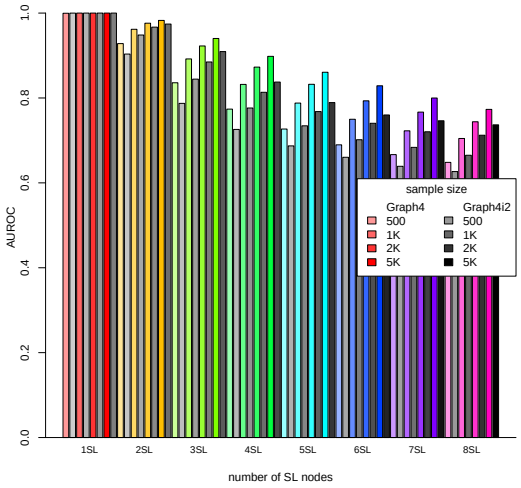

(e) Performance Between Graphs (a) and (c)

Figure 6.13: **Performance is affected by inhibition in graphs.** The AUROC values for simulations of multivariate normal distributions based on graph structure containing only inhibitions in the Graph structure yielded consistently higher performance across parameter values in 10,000 simulations. A combination of activating and inhibiting relationships had lower performance but was more similar to the activating graph.

6.2.3 Synthetic Lethality across Graph Structures

While synthetic lethal genes are distinguishable in principle from those highly positively correlated with them (as shown by ROC analysis), they are not necessarily distinguished as reflected by low specificity and high false positive rates in poorly performing simulations throughout this section. The negative correlations are not subject to the same issue, they sometimes perturb the correlation structure between synthetic lethal partner genes making it difficult to detect many of them. Thus far, synthetic

lethal genes have been selected randomly which is a limited approach. To examine the impact of pathway relationships in more more detail, specific genes will be selected to be synthetic lethal within a network. Replicate simulations were performed for synthetic lethal detection with a fixed synthetic lethal gene, in contrast to previous investigations (randomly selecting synthetic lethal genes). This investigation was performed to demonstrate the impact of these genes being synthetic lethal in the detection of neighbouring genes in the pathway network, under graph structure activating and inhibiting relationships.

For instance, detection of a synthetic lethal gene in an activating graph structure (as shown in Figure 6.14a) is straightforward: the χ^2 values across simulations are clearly distinguishable from non synthetic lethal genes (shown in Figure 6.14c). A small number of simulations were performed for each gene being designated as synthetic lethal. In each case (of each gene being the synthetic lethal partner), the synthetic lethal gene was detectable with highest χ^2 value, being distinguishable amongst 20,000 genes including the highly correlated graph network (as shown in Figure K.5).

This is consistent with previous observations that SLIPT performed optimally for a single synthetic lethal partner in this network (in Figure 6.9). Despite optimal performance in a ROC curve irrespective of detection threshold, many of the highly correlated genes would be detected as false positives using a conventional p-value threshold (even if adjusted by {glsFDR) from a χ^2 test with 4 degrees of freedom as performed by SLIPT (as described in Section 3.1). In particular, the genes that are adjacent to the synthetic lethal gene "D" within the graph structure exhibited high test statistics across simulations which would often be reported as false positives (as shown in Figure 6.14c). This is not specific to example of gene "D", with the neighbouring genes exhibiting higher χ^2 test statistics for each gene in the network when it is designated as the synthetic lethal partner (as shown in Figure K.5).

Thus the synthetic lethal signal propagates from the true synthetic lethal gene throughout the network such genes nearer to the true synthetic lethal gene (more highly correlated) have higher test statistics and are more likely to be detected by SLIPT as false positives. This tendency for adjacent genes to be detected as synthetic lethal false positives is consistent with the synthetic lethal pathways being more concordant between SLIPT in TCGA data (TCGA, 2012) and the siRNA screen (Telford *et al.*, 2015) than individual gene results (in Chapter 4). False positive genes are therefore still more likely to be involved in a synthetic lethal pathway by being correlated with a true synthetic lethal gene and synthetic lethal pathways are likely to have

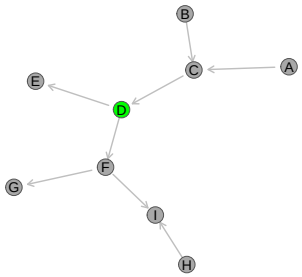

(a) Activating Graph

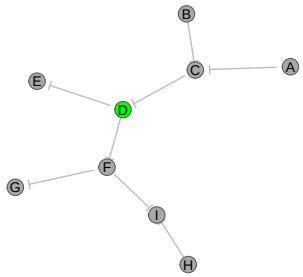

(b) Inhibiting Graph

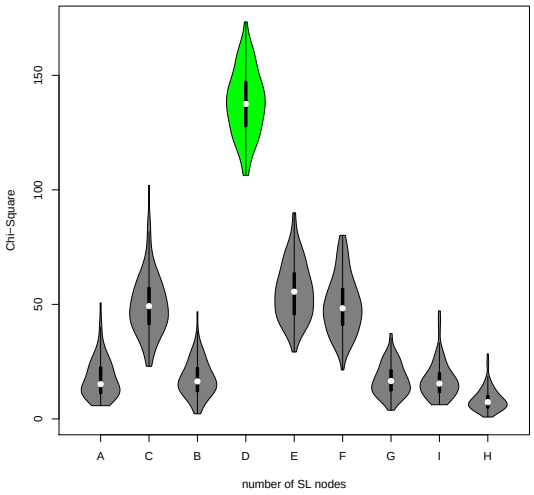

(c) χ^2 distribution for Activating Graph

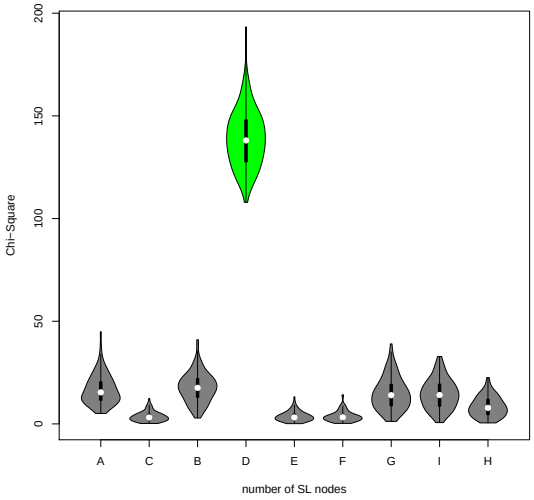

(d) χ^2 distribution for Inhibiting Graph

Figure 6.14: **Detection of Synthetic Lethality within Graph Structure with Inhibitions.** The gene "D" was designated to be synthetic lethal and the χ^2 value from SLIPT was computed for each gene across each graph structure. The χ^2 values were computed in 100 simulations of datasets of 20,000 genes including the graph structure and 1000 samples. Adjacent genes exhibited lower χ^2 values with inhibiting relationships.

many genes detected by SLIPT giving a consensus of evidence, supporting the pathway over-representation approach in particular which may account for how it differs from pathway metagenes. Furthermore, SLIPT is still viable to detect true synthetic lethal partners or prioritise those most likely to be experimentally validated since those with the strongest support (i.e, higher χ^2 values and more significant p-values) are more likely to be the underlying synthetic lethal gene.

In contrast to an activating graph (Figure 6.14a), the immediately adjacent genes in an inhibiting graph (Figure 6.14b) had neither an elevated χ^2 test statistics indicating synthetic lethality nor a significant inverse effect (as shown in Figure 6.14d). Similar simulations were performed a graph structure with inhibiting relationships within a dataset of 20,000 genes. The adjacent genes to the synthetic lethal gene "D" did not have elevated χ^2 values and therefore true synthetic lethal partners were highly distinguishable from non synthetic lethal genes with inhibiting relationships. This was not specific to "D" and was shown across any gene in the graph structure if it were designated to be the synthetic lethal partner of the query gene (shown in Figure K.6). This is consistent with the detection of many genes involved in kinase signalling, gene regulation, and other known cancer pathways (in Chapter 4) which frequently have inhibitory steps. These results support SLIPT as an appropriate approach to distinguish synthetic lethal partners in biological pathways, including those relevant to cancer growth and inhibition.

However, it should be noted that the 2$^{\text{nd}}$ degree neighbours of the synthetic lethal gene still exhibited moderate χ^2 values (and are moderately correlated with the synthetic lethal gene). It is still possible for these to be detected as false positives as previously described for an activating graph structure although the presence of inhibitory relationships (and negative correlations) further increases the differences in test statistics for correlated genes and underlying synthetic lethal partners as shown by the extreme example (in Figure K.6).

These findings are consistent with simulations in a graph containing a combination of activating and inhibiting relationships which exhibits a either of these χ^2 profiles depending on which gene is synthetic lethal and the relationships to adjacent genes (as shown in Figure K.7). Note that in this case, the synthetic lethal gene is distinguishable and inhibitory relationships within this graph structure make it easier to detect underlying synthetic lethal genes with SLIPT by a more highly significant χ^2 test. This contrasts with randomly selecting multiple synthetic lethal genes (in Figure 6.13) where the performance of SLIPT was impeded by the inhibitory relationships between synthetic lethal partners in this graph structure. Therefore the random synthetic lethal genes selected previously with negative correlations between them which had poor performance are likely to have created an artifact in the simulation results as they are biologically implausible and constrain the synthetic lethal simulation procedure

The results with one synthetic lethal partner were sufficient to infer the impact of synthetic lethal partners within pathways on neighbouring (correlated) genes. However,

it is plausible that the synthetic lethal signatures in expression data would propagate through a network with multiple synthetic lethal partners as sources, provided that the correlations between synthetic lethal partners is biological feasible. These simulations were performed on a correlated graph structure within a larger gene expression dataset of 20,000 genes (as performed in Sections 3.3 and 6.2.4), a feasible number for a full human gene expression dataset, and as such are comparable to the findings below.

6.2.4 Performance within a Simulated Human Genome

As noted in Section 6.2.1.1, the high proportion of synthetic lethal partners in small networks made accurately assessing the performance of SLIPT with higher numbers of true partners to detect (and fewer true negatives) difficult. Similarly, adding more true negative genes in previous simulations increased the performance of SLIPT, particularly the specificity to reduce the number of false positives (as shown in Sections 3.3 and 6.1). Building on these findings, here the graph structures (as used in Section 6.2.1) of genes with correlations from sampling a multivariate normal distribution were included in a larger simulated dataset of 20,000 genes. This simulation procedure serves to test the performance of SLIPT at detecting synthetic lethal partners within correlated graph structures (of a synthetic lethal pathway) in the context of biologically feasible numbers of genes.

The simulations performed in Section 6.2.1.1 were replicated within a dataset of 20,000 genes with the rest being composed on non synthetic lethal genes without correlation structure. The aforementioned issue with specificity in a higher number of underlying synthetic lethal genes did not occur in a simple graph structure (as shown in Figure 6.15). For such a small graph module of highly correlated genes within a gene expression dataset, detection of synthetic lethal genes within the network by SLIPT and distinguishing these from the larger dataset performed well across parameter values. In this case, a reduction in sensitivity was the cause of poorer performance as a higher number of non synthetic lethal genes were detected as true negative with a low false positive rate and high accuracy. This further supports the use of stringent χ^2 p-value thresholds (adjusted by {glsFDR) for testing for synthetic lethality in gene expression data across the number of genes in human and cancer data.

In a direct comparison with simulations in the graph structure alone (as performed in Section 6.2.1.1), detection of synthetic lethality with SLIPT performs consistently better in a larger dataset with many true negative genes to detect (as shown in Figure 6.16). This is a desirable property of the SLIPT methodology as it has a high

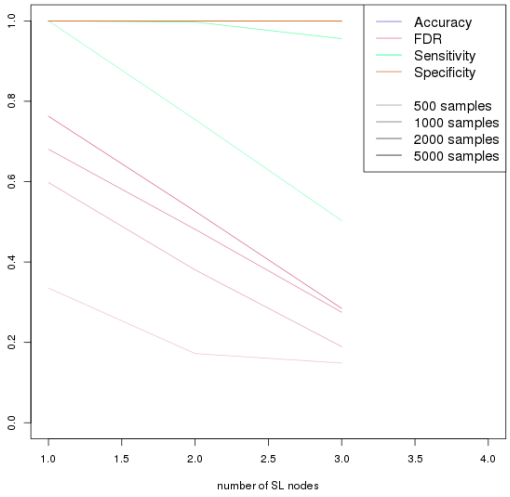

(a) Statistical evaluation

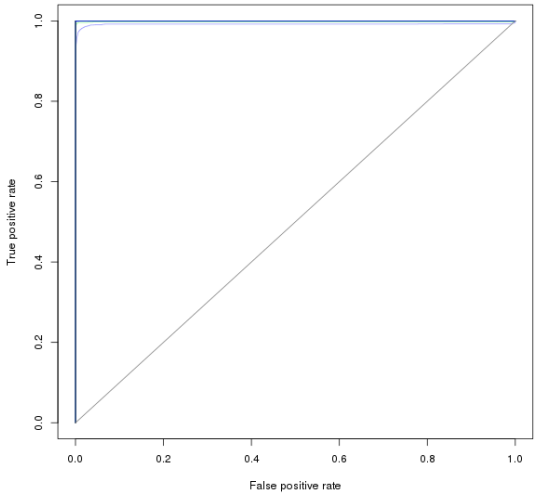

(b) Receiver operating characteristic

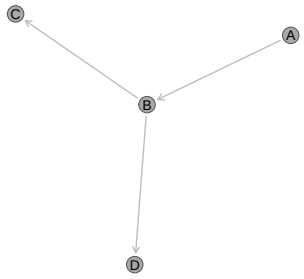

(c) Graph Structure

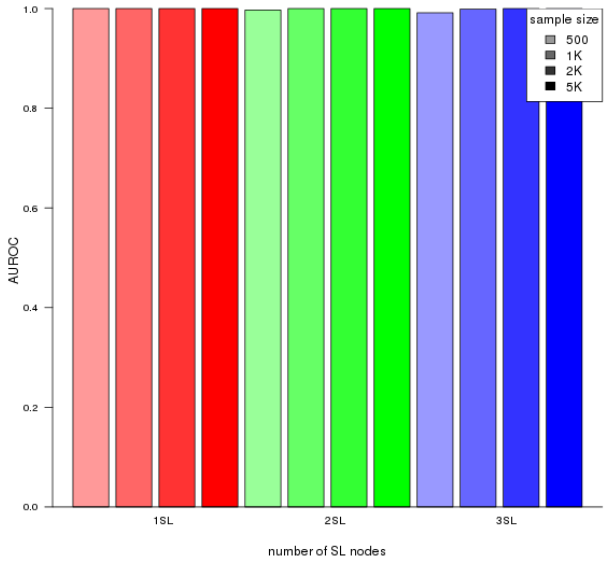

(d) Statistical performance

Figure 6.15: **Performance of simulations including a simple graph.** Simulation of synthetic lethality was performed sampling from a multivariate normal distribution (without correlation structure apart from the graph shown). Performance of SLIPT was high across parameters for detecting synthetic lethality in the graph structure within a larger dataset. The sensitivity decreases for a greater number of true positives to detect but the specificity remains high with a low false positive rate.

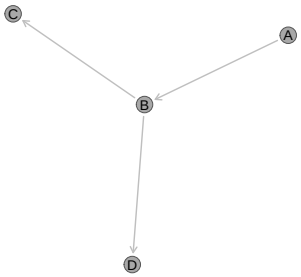

(a) Diverging Module

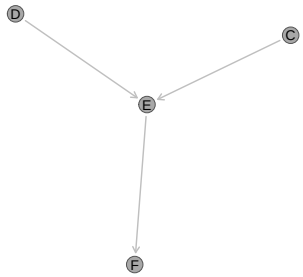

(b) Converging Module

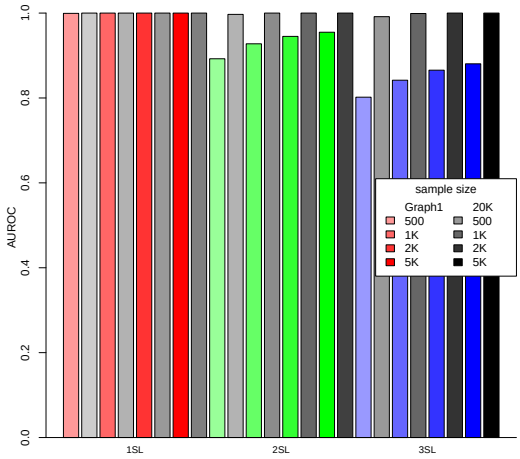

(c) Performance in Diverging Module

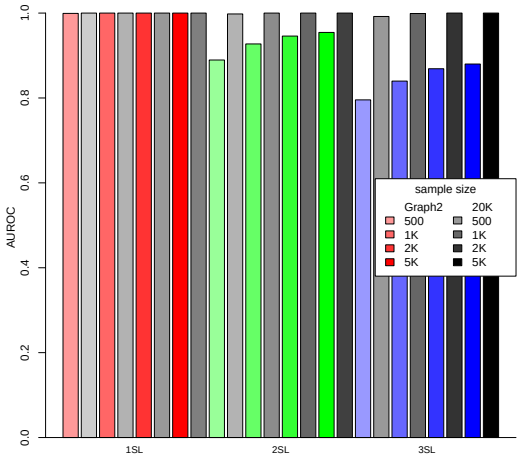

(d) Performance in Converging Module

Figure 6.16: **Performance on a simple graph improves with more genes.** Simulations were performed with each of the graph structures to detect synthetic lethal partners within them. In either structure, performance of detection in a dataset containing on the graph structure (in colour) was lower than testing the graph structure within a larger dataset of non synthetic lethal genes (without correlations).

specificity and low false positive rate. SLIPT is therefore applicable to large gene expression datasets where these are important considerations since the number of negative genes to correctly identify often vastly outnumbers the number of positive genes to detect.

This increase in performance with more negative genes to detect does not necessarily apply in an inhibiting graph structure. While an increased performance for an activating graph was replicated in this case, the performance of simulations of an en-

tirely inhibiting graph structure did not improve within a larger dataset (as shown in Figure **??**). There is cause for concern since the biological pathways commonly contain inhibiting relationships (and inverse correlations), however, they are rarely as frequent as modelled here. It is reassuring that the performance in the inhibiting graph structure is comparable to simulations of the graph structure in isolation rather than diminished. It is expected that the findings based on simulations of genes with pathway structures in smaller datasets (as described in Section 6.2.1) will be relevant to larger datasets since the simulation results in these perform comparably or higher with more non synthetic lethal genes to distinguish from them even with inhibitory relationships within the graph structure

Performance of synthetic lethal detection of SLIPT in graphs structures with inhibitions included in a larger dataset of non synthetic lethal genes did not necessarily diminish to the level of the graph structure simulated alone. In some cases (as shown in Figure 6.17), the performance of an inhibitory graph structure was consistently elevated when included within a larger data. However, these did not perform as well as the equivalent activating graph structures within a similar dataset.

This poorer performance is unlikely to occur due to highly negatively correlated genes being false positives as they will be positively correlated with the query gene if they are negatively correlated with a synthetic lethal partner (i.e., within a synthetic lethal pathway). The SLIPT procedure performs well at distinguishing these, as previously shown (in Sections 3.3.2.2 and 6.1.1.1). These false positives will also be a minority amongst a larger dataset of non synthetic lethal genes without correlation to the query or synthetic lethal genes.

It more likely that the poorer performance stems from negative correlations between synthetic lethal genes which makes them more difficult to individually detect (as observed in Section 6.2.2). As discussed in Section 6.2.3, this is likely an artifact of the simulation procedure selecting random synthetic lethal genes which may be biologically implausible (e.g., strong inhibitory relationships between them). Therefore the poorer performing inhibiting graphs within larger datasets are not cause for concern as the cases where SLIPT performs poorly are combinations of simulated synthetic lethal genes which are unlikely to occur within biological pathways. Furthermore the simulation procedure has used included higher-order synthetic lethal to produce the weakest signal of synthetic lethality for individual partner genes and these are still detectable by SLIPT.

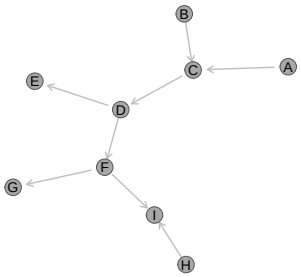

(a) Graph Structure

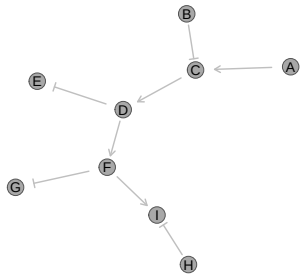

(b) Inhibiting Structure

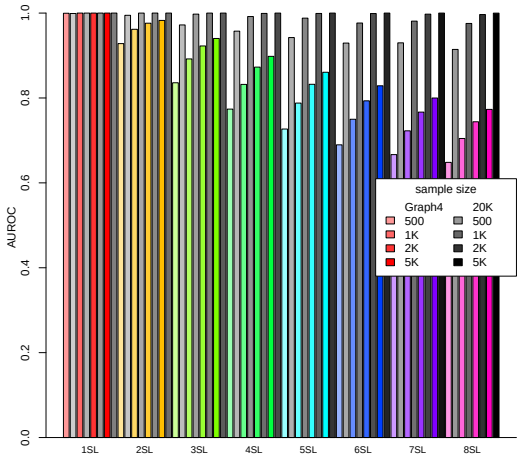

(c) Performance in Graph

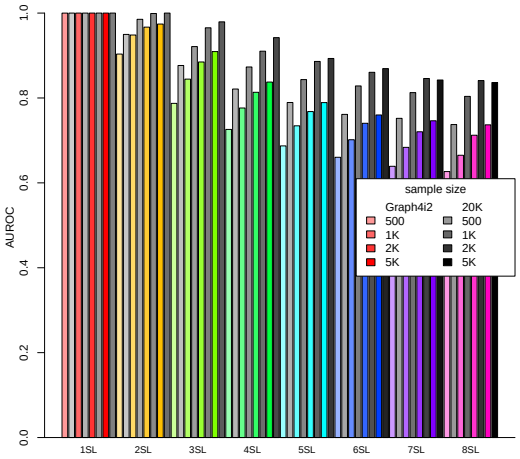

(d) Performance with Inhibitions

Figure 6.17: **Performance on an inhibiting graph improves with more genes.** Simulations were performed in a graph structure with activating and inhibiting relationships to detect synthetic lethal partners within them. In contrast to an activating graph, performance of detection in a dataset containing only the graph structure (in colour) was as much lower than testing the graph structure within a larger dataset of non synthetic lethal genes (without correlations) in an inhibiting graph structure with negative correlations.

6.3 Simulations in More Complex Graph Structures

As shown in Figure K.10, sensitivity declines over a greater range for the number of synthetic lethal partners in a larger network with a tradeoff with specificity. However, the accuracy declines for greater numbers of synthetic lethal partners and the false positive rate peaks at intermediate values. In this range, difference between simulations varies with greater sample size. The AUROC results were similar for other more

complex graph structures (as shown in Figures K.8 and K.9). These graphs performed similarly to each other, although they had differences from Figure K.10 in their sensitivity and specificity at an adjusted ({glsFDR) p-value threshold. This difference may stem from different ratios of synthetic lethal and non-synthetic lethal genes to detect, since the latter graphs (in Figures K.8 and K.9) had half the total genes to that shown in Figure K.10.

However, the graph structures (of similar size) were highly distinct and yet had similar performance profiles across parameters. Therefore SLIPT is robust across pathway structures and is more affected by the number of genes to detect and the proportion of them out of those tested. As such findings from previous simulations in similar correlation structures (in Section 3.3) should be applicable to expression data with more complex correlation structures such as those occurring in biological pathways. Specifically, synthetic lethal partners are distinguishable from closely correlated genes in the context of a biological pathway network both irrespective of thresholds (shown by ROC) and with the sensitivity and specificity of p-value thresholds (adjusted by {glsFDR) as used for SLIPT (in Chapters 4 and 5).

The findings for inhibitory graph structures were replicated with larger more complex graph structures with inhibiting relationships and more synthetic lethal genes to detect (shown in Figures K.15–K.14). In each graph structure, simulations entirely with inhibiting relationships (Figures K.15, K.11, and K.13) had higher performance than the equivalent graph with entirely activating relationships (Figures K.10, K.8, and K.9) or a combination of activating and inhibiting relationships (Figures K.16, K.12, and K.14). As previously observed (in Figures K.8 and K.9), the proportion of underlying synthetic lethal genes to detect had a greater impact on performance of detection with SLIPT than the specific structure of the genes which was replicated with inhibiting states (in Figures K.11 and K.13) and combinations with a similar proportion of negative inhibitions (in Figures K.12 and K.14). While the presence of negative correlations subtly affects the performance of SLIPT, the methodology is robust across the exact structures of genes and is therefore applicable to detecting synthetic lethal genes in a range of (synthetic lethal) biological pathways with different structural relationships.

6.3.1 Simulations over Pathway-based Graphs

Thus far simulations of synthetic lethality in gene expression with correlation structures have used simple blocks of correlated genes (as used in Section 3.3) or derived from artifically constructed graph structures (as used in Section 6.2). While these

are sufficient to make inferences on the impact of correlation structure, it remains to be shown whether these findings are reproducible in the complexity of the biological network structure. Specifically, SLIPT was tested on simulated data with known underlying simulated synthetic lethal partners (as described in Section 3.2.2) with multivariate normal correlation structure derived from biological pathways (as described in Section 3.4.2).

The Reactome pathway structure for the PI3K cascade (as used extensively in Chapter 5) was used to demonstrate the simulation procedure for detecting synthetic lethality in the graph structure of a biological pathway. It is appropriate to do so since this pathway has clear directionality and signalling pathways were among those identified to be synthetic lethal candidates (in Chapter 4). The PI3K pathway having 138 genes is also of a moderate size and complexity compared to other biological pathways which is therefore suitable for comparison to previous graph structures of a similar scale (50–100 genes) with the complexity of a characteristic of a biological pathway.

The performance of synthetic lethal detection with SLIPT in simulated expression data based on the Reactome PI3K pathway (as shown in Figure 6.18) was concordant with previous findings. SLIPT had high performance at detecting a low number of synthetic lethal genes with poorer performance for high numbers of synthetic lethal genes or lower sample sizes. In particular, the performance of simulations in the PI3K pathway was highly resembled the simulation results for constructed graphs of similar scale and complexity (as shown in Figures K.8 and K.9). Using thresholds based on the χ^2 p-value (adjusted by {glsFDR), simulations in the biological PI3K pathway had a higher sensitivity and lower specificity. While the performance decreases for more synthetic lethal genes to detect within the simulated PI3K pathway, this primarily involves a reduction in sensitivity to detecting underlying synthetic lethal genes rather than false positives as the false positive rate decreases, the accuracy increases, and the specificity is relatively unperturbed (being more dependent on sample size). Thus SLIPT is stringent in biological graph structures and appropriate for detection of synthetic lethal genes in complex correlation structures in gene expression data involving biological pathways.

These simulations were replicated in the larger and more complex , one of the most well supported synthetic lethal pathways with loss of *CDH1* in cancer (in Chapters 4 and 5). This pathway showed similar relationships between sensitivity, specificity, and false positive rate with number of synthetic lethal partners and sample size (as shown in Figure K.17). While the overall performance was lower than for smaller networks

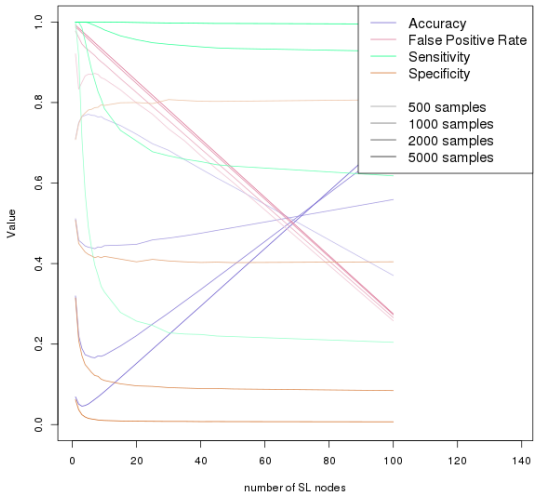

(a) Statistical evaluation

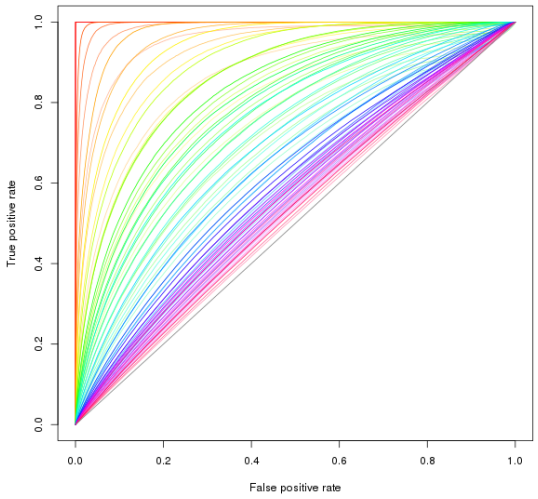

(b) Receiver operating characteristic

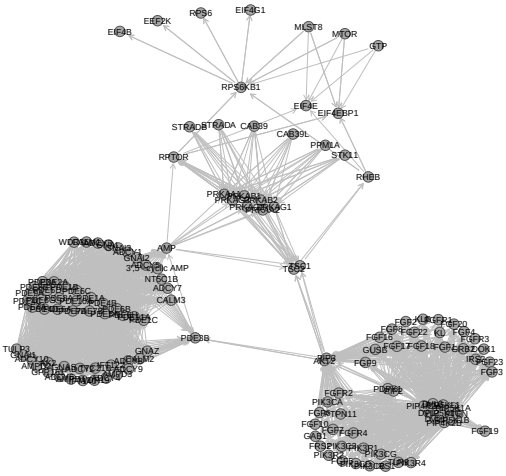

(c) Graph Structure

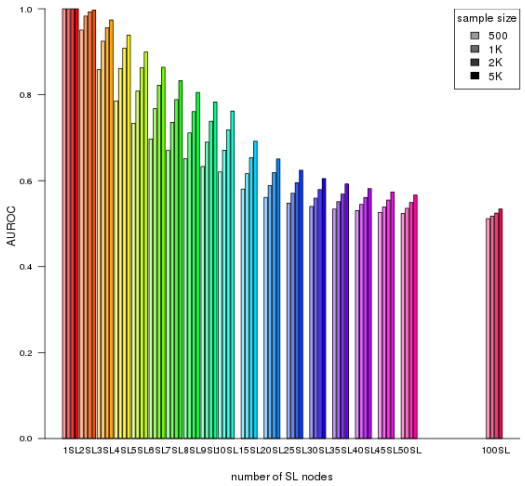

(d) Statistical performance

Figure 6.18: **Performance of simulations on the PI3K cascade.** Simulation of synthetic lethality was performed sampling from a multivariate normal distribution based on the Reactome PI3K cascade. Performance of SLIPT was high across parameters for detecting synthetic lethality in the graph structure within a larger dataset. The performance decreases for a greater number of true positives to detect but the accuracy increases with a low false positive rate.

structures, many of the findings from previous networks were replicated in a larger more complex biological network. In the $G_{\alpha i}$ signalling pathway, SLIPT performed well for

detecting low numbers of synthetic lethal genes and was highly stringent against false positives for higher numbers of synthetic lethal genes.

6.3.2 Pathway Structures in a Simulated Human Genome

Simulations were also performed with graph structures from biological pathways included in a larger dataset to simulate gene expression data of the scale typical for human and cancer studies. These simulations (as discussed in Section 6.2.4) have a higher specificity and therefore performance of SLIPT for detecting synthetic lethal genes was higher. The simulated PI3K pathway (as shown in Figure 6.19), is no exception with high performance across parameter values, remaining high up to many genes. While the sensitivity decreases for high numbers of synthetic lethal genes to detect within the PI3K pathway, the SLIPT methodology remains accurate with high specificity in a large simulated gene expression dataset.

Therefore the SLIPT is a highly stringent approach suitable for application to detecting synthetic lethal genes and pathways within highly complex expression data with biological pathway structure. In particular, the poorer performing simulations were highly stringent with low false positive rates which are an important consideration given the number of non synthetic lethal genes to distinguish in a gene expression dataset. The enrichment of true synthetic lethal partners makes SLIPT valuable for triage of candidates interacting synthetic lethal partners for further validation and for pathway analysis.

The performance of simulation of synthetic lethality within a biological pathway (e.g., the example of the PI3K cascade) was markedly higher in the context of a larger dataset of thousands of genes. As shown in a direct comparison with the graph structure alone (in Figure 6.20c), performance was consistently higher across parameters in pathways of biological complexity from the Reactome database (Croft *et al.*, 2014) such as PI3K cascade). These findings were also replicated in the larger $G_{\alpha i}$ signalling pathway (shown in Figures K.18 and 6.20d).

The biologically complex graph structures based on the Reactome pathway use activating relationships to test synthetic lethal detection with SLIPT in the context of complex correlation structures. Inhibiting relationships were not used, these annotations are not provided in the Reactome database (Croft *et al.*, 2014). However, these investigations with pathway based graph structures are informative of the findigns in constructed graphs (as used in Section 6.2) being relevant to gene expression data containing real correlated pathways. Furthermore previously comparisons between sim-

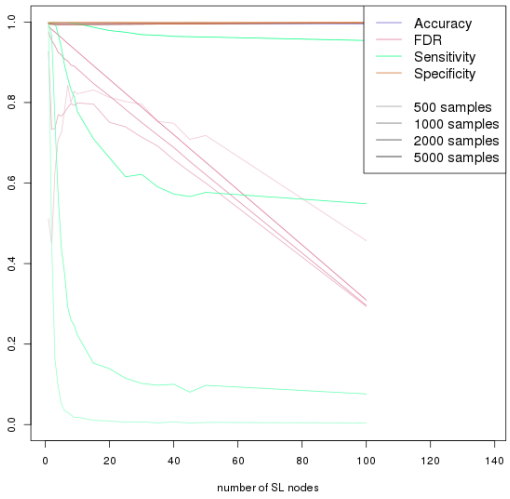

(a) Statistical evaluation

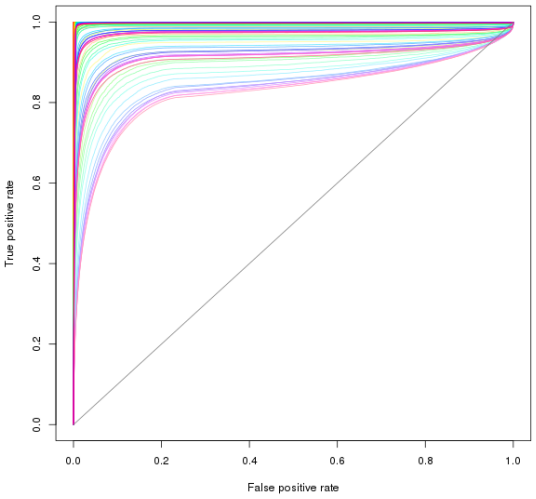

(b) Receiver operating characteristic

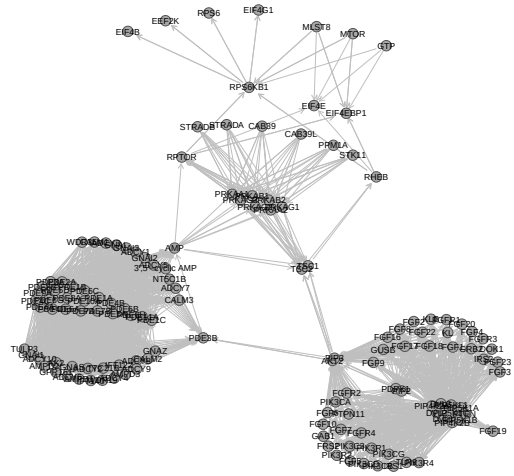

(c) Graph Structure

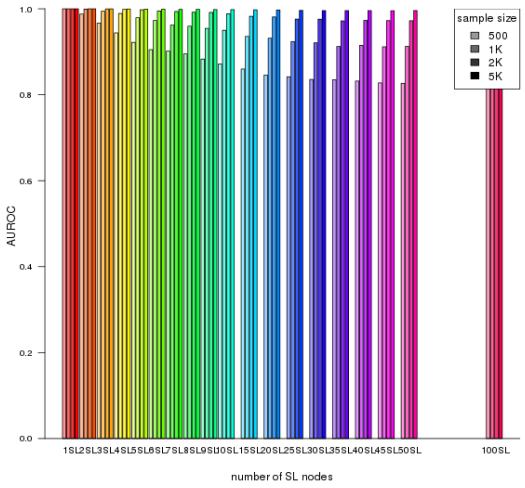

(d) Statistical performance

Figure 6.19: **Performance of simulations including the PI3K cascade.** Simulation of synthetic lethality was performed sampling from a multivariate normal distribution (without correlation structure apart from the Reactome PI3K cascade). Performance of SLIPT was high across parameters for detecting synthetic lethality in the graph structure within a larger dataset. The sensitivity decreases for a greater number of true positives to detect but the specificity remains high with a low false positive rate.

ulations with inhibiting relationships indicate that the performance of synthetic lethal

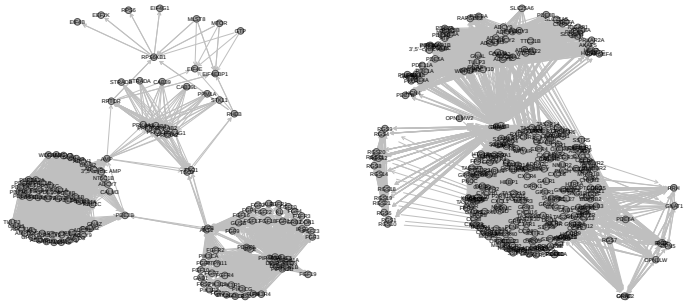

(a) The PI3K cascade (b) G signalling

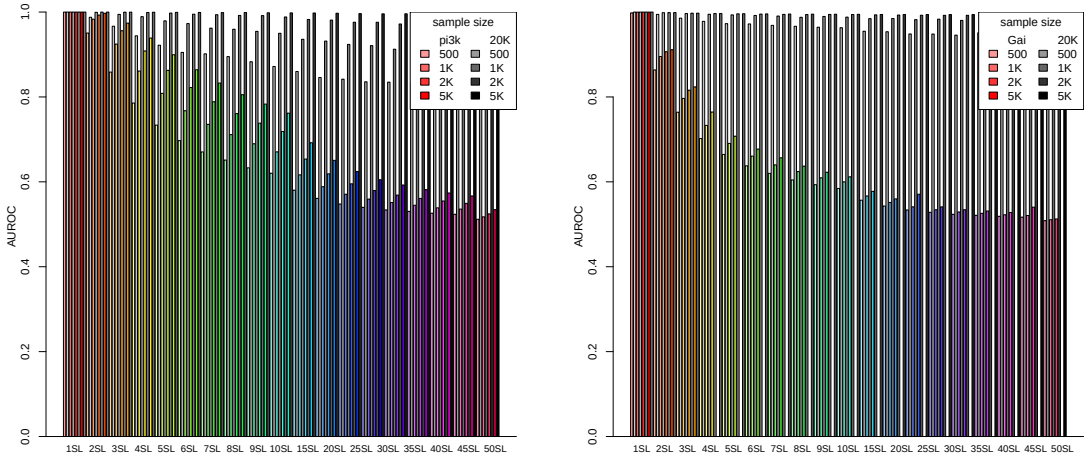

(c) Performance in the PI3K cascade (d) Performance in G signalling

Figure 6.20: **Performance on pathways improves with more genes.** Simulations were performed in a graph structures for the PI3K cascade and $G_{\alpha i}$ signalling pathways structures to detect synthetic lethal partners within them. As for constructed graphs, performance of detection in a dataset containing only the graph structure (in colour) was as much lower than testing the graph structure within a larger dataset of non synthetic lethal genes (without correlations) for both graphs of biological complexity.

detection in an equivalent graph structure with inhibitory relationships will likely be higher.

Negative genes (non synthetic lethal) inversely correlated with the underlying synthetic lethal partners will be distinguishable by SLIPT with high specificity. Since synthetic lethal genes are detectable will reasonable performance in large scale simulated gene expression data and highly (positively) correlated genes in pathway structures,

these findings serve as a conservative lower estimate for SLIPT detecting synthetic lethal genes within a synthetic lethal biological pathway in empirical data. While synthetic lethal genes are distinguishable from correlated genes to varying extents in simulations, false positives are also more likely to be within the same (synthetic lethal pathways). Therefore SLIPT is both effective at triage of synthetic lethal candidates within a biological pathway and at identifying synthetic lethal pathways in high dimensional gene expression data.

6.4 Discussion

6.4.1 Simulation Procedure

Simulations have been performed to assess the performance of the SLIPT methodology (as described in Section 3.1 and with modifications) for detecting known underlying synthetic lethal partners of a query gene. These simulations support the the findings in empirical data (in Chapters 4 and 5) by addressing whether the methodology used to generate them is accurate or has desirable statistical performance in controlled simulated conditions. These investigations include adjusting parameters such as the numbers of synthetic lethal genes which were known in empirical data to assess the performance of the SLIPT methodology across simulation parameters and characterise the datasets for which SLIPT performs well. Simulation and statistically modelling also enables comparison of the SLIPT methodology to other statistical approaches to synthetic lethal detection in expression data.

These simulations are based on a statistical model of synthetic lethality (as described in Section 3.2.1) which was designed stringently to ensure that if synthetic lethality is detectable in the simulated datasets it would also be detectable by the same methodology in empirical expression data. The model of synthetic lethality made conservative assumptions such as the low threshold of expression for gene function or the inclusion of cryptic higher-order synthetic lethality (when testing pairwise). These assumptions decrease the likelihood that synthetic lethal signatures would be detectable in expression data. Thus it is reassuring that synthetic lethality is still detectable in under many simulation parameters as the performance of SLIPT would be expected to be higher were these assumptions to be violated in empirical data.

The simulation procedure (as described in Section 3.2.2) is designed as a computational pipeline with arguments passes to scripts. The SLIPT methodology and simulation of expression from graph structures were both used as R (R Core Team, 2016)

software packages developed and released for this project (as described in Section 3.5). This design ensures that the simulations can be robustly applied across parameters with consistency between simulations apart from the differences discussed. The simulation procedure is also flexible to simulating other datasets, including synthetic lethal relationships and pathway correlation structures, should these be relevant to future investigations or bioinformatics tool development. The computational pipeline is also compatible with parallel computing and made use of High Performance Computing (HPC) infrastructure provided by the New Zealand eScience Infrastructure (NeSI) using the Simple Linux Utility for Resource Management (Slurm) submission system (as described in Section 2.5.3). This parallel computing pipeline enabled extensive investigations into synthetic lethality in simulated data, including approximately 2 million cpu-hours on NeSI.

6.4.2 Comparing Methods with Simulated Data

Attempts were made to implement alternative synthetic lethal detection approaches such as linear regression and the BiSEp R package (discussed in Section 6.1). However, those tested were ineffective at detecting synthetic lethality in multivariate normal simulated data in comparison to SLIPT. While some of the published synthetic lethal detection methods (Jerby-Arnon *et al.*, 2014; Lu *et al.*, 2015) did not provide reproducible software releases for direct comparison, some of the central assumptions used in their design were tested by the statistical methods considered for synthetic lethal detection in expression data.

Another consideration is that BiSEp takes considerably more time to compute predictions than SLIPT or χ^2 which limited the number of simulations that were feasible and made it difficult to apply across parameters in the simulation pipeline (even when using supercomputing infrastructure as discussed in Section 2.5.3). The computationally intensive nature of the BiSEp procedure does not appear to be the issue for detecting synthetic lethal genes in TCGA data or simulations, although it has made more extensive simulations challenging. Rather, BiSEp is not suitable in either case since the TCGA data is normalised with `voom` (Ritchie *et al.*, 2015) and simulated data is generated by sampling from a multivariate normal distribution. In either case, even subtle bimodal signatures in expression data were not consistently detectable or sufficient to detect synthetic lethality.

The BiSEp methodology may perform better on other data types but it cannot be directly compared with the results for SLIPT throughout this thesis which have used

normalised or (multivariate) normally distributed data. Since it requires bimodal distributions, BiSEp is not suitable for stringently normalised expression data nor would it be expected to perform on (ranked) pathway metagenes. Thus SLIPT represents a distinct approach more suitable for these data types whereas BiSEp may be applicable to other applications in which bimodal distributions are more frequent.

This investigation also demonstrates that implementing scientific software from other research groups is not a trivial exercise, even when released as an open-source R package. Therefore, the above results were used to evaluate SLIPT and compare it to other statistical rationales. An comprehensive comparison to contemporary synthetic lethal detection approaches (and those released in the future) or further benchmarking is left to an impartial researcher to evaluate. The above findings show that the SLIPT approach is able to detect synthetic lethal genes in simulated data with comparable or better performance than a range of distinct statistical techniques and was appropriate for use throughout this thesis.

6.4.3 Design and Performance of SLIPT

The simulation procedure using sampling from a multivariate normal distribution was used throughout the majority of the simulation investigations in this thesis. This approach has the advantages of emulating the continuous normalised expression data used for gene expression analysis and enables the simulation of correlation structures (as discussed in Section 3.3). These simulations scaled to datasets of comparable scale to those used in gene expression anlaysis with thousands of genes. The SLIPT methodology was shown to perform robustly across large numbers of genes and simple correlation structures. This includes high specificity against genes positively correlated with the query gene for which the directional SLIPT methodology more suited to distinguishing synthetic lethal genes from than the χ^2 test without directional criteria on the number of samples observed.

These findings were expanded upon in this chapter. Specifically, different quantiles were compared for SLIPT and the χ^2 test. These approaches using threshold based discrete gene function were compared to the Pearson correlation without loss of the continuous expression data. The 3-quantiles for SLIPT (as described in Section 3.1) were optimal for both SLIPT and the χ^2 alone. In addition to being optimal for estimating the significance of synthetic lethal interactions, these quantiles were also optimal for the directional criteria of SLIPT since this method outperformed the χ^2 test and was the most different at the 3-quantile. As previously, noted this difference

was more pronounced with positively correlated genes (with the query gene) for which the specificity of SLIPT improves and was replicated in large datasets with thousands of genes as occur in human expression data. These results were not simply due to sufficient samples for significant p-values since the performance as determined by AUROC analysis is independent from significance thresholds. This indicates that the SLIPT methodology (as it has been used in Chapters 4 and 5) is optimal and the parameters used to design it were appropriate.

Both discrete functional approaches (SLIPT and χ^2) were able to outperform negative correlation which supports their use. In particular, this result addresses the concern that arbitary thresholds of low and high gene function (as used by SLIPT) lose useful data by compressing the spectrum of gene expression into categorical data. However, this does not impede the performance of SLIPT and can reduce statistical if the quantiles used are optimal. The poorer performance of correlation-based detection of synthetic lethality also indicates affirms the concept of gene function for synthetic lethality being qualitative, that is expression must be sufficient for cell viability and higher expression is not necessarily higher function (as this is not the case for all genes). Furthermore, the finding that negative correlation outperforms positive correlation is also consistent with co-expression being a poor predictor of synthetic lethality compared to other approaches (Jerby-Arnon *et al.*, 2014), supporting the claims of Lu *et al.* (2015).

Compared with SLIPT, neither correlation approaches nor bimodality signatures were suitable for detecting synthetic lethality in expression data. The correlation-based approaches make assumptions about the relationship between gene expression and function which do not necessarily hold for all genes. Similarly, the bimodal approach is not appropriate for normalised data since deviations from a normal distribution have already been used for ensuring data quality, as is common practice for RNA-Seq data. Other approaches were continuous data such as fitting linear models are likely to be prone to similar issues and not perform as well as SLIPT. However, it is possible that these may be improved with conditioning on known synthetic lethal partners with multivariate regression or Bayesian priors. Similarly, synthetic lethal detection could be performed by iteratively conditioning upon the strong candidate from previous analysis. These approaches may be able to better circumvent the issues of high-order synthetic lethality and multiple testing.

Nevertheless, the above findings are sufficient to assess the performance of SLIPT and present an effective straightforward approach to synthetic lethal detection in gene

expression data. Further development of linear models, Bayesian inference approaches, or comparison to existing synthetic lethal approaches (e.g., machine learning) remain as future directions. Developing and testing more sophisticated statistical approach to synthetic lethal detection may benefit from the concepts discussed with regard to the relatively simple SLIPT methodology. Similarly, further comparisons and benchmarking of SLIPT against other computational approaches to synthetic lethal detection in gene expression data is more suitable for an independent researcher and the `slipt` R package has been released (as described in Section 3.5) for this purpose, in addition to further application in research.

6.4.4 Simulations from Graph Structures

The simple correlation structures (as used in Section 3.3) were expanded upon to simulate correlated genes based on graph structures using the multivariate normal simulation procedure on correlation structures generated from grahp structures (as described in Section 6.2). These simulations enable further investigations into te performance of SLIPT in the context of more complex correlation structures. The simulation of expression from network structures is widely applicable to simulating pathway expression data and as such the `graphsim` R package has been released (as described in Section 3.5).

These investigations show that SLIPT performs robustly across datasets with different correlation structures, including those derived from graphs with the complexity of biological pathways. The SLIPT methodology was able to detect synthetic lethal genes within synthetic lethal pathways across many graph structures. This methodology performed particularly well with synthetic lethal pathways in the context of a larger dataset with a high specificity which supports SLIPT as a stringent approach to synthetic lethal detection in highly dimensional gene expression data. Together these results support the use of SLIPT in biological gene expresssion data since it is able to detect synthetic lethal genes in highly complex correlation structures.

Similarly, the inclusion of inhibitory relationships in graph structures was shown to increase the performance in simple networks supporting SLIPT being applicable to biological data in which these relationships are common. While these results were not replicated in more complex inhibitory graph structures, this is likely an artifact of the simulation procedure (which randomly selects synthetic lethal genes) generating biologically implausible combinations of synthetic lethal genes which are difficult to detect. When the test statistics in simulations with a synthetic lethal gene were examined in

more detail, the test statistics of the synthetic lethal gene were consistently higher and distinguishable from nearby genes in the graph structure. In contrast to previous concerns with inhibiting relationships, these differences were more pronounced with genes which had inhibitory relationships with synthetic lethal genes. While distinguishable from nearby genes in a pathway structure, the genes correlated with synthetic lethal still had higher test statistics than more distant genes (similar to observations with correlated genes in Section 3.3).

In addition to being able to detect synthetic lethal genes in a pathway, the proximal genes in a pathway are most likely to be false positives and therefore SLIPT is also able to detect synthetic lethal pathways. Therefore SLIPT identifies genes which are likely to be constituent of a synthetic lethal pathway and is more likely to rank underlying synthetic lethal genes with greater significance. Together these findings support the use of SLIPT throughout this thesis, further application of SLIPT, and further development of such strategies for synthetic lethal detection. Similarly, the simulation procedures developed and demonstrated for examining synthetic lethal detection in expression data using graph structures is amenable to further development and investigations into pathway structure in expression data such as predicting biological pathways from expression data or the impact of pathways on differential expression analyses.

6.5 Summary

A statistical model and simulation procedure has been developed to test the performance of the SLIPT methodology in controlled conditions, using multivariate normal distributions. This simulation procedure has been developed into a computational pipeline which was able to test the statistical performance (using stringent assumptions) of SLIPT across many parameters and compare it to alternative synthetic lethal detection strategies. The SLIPT methodology performs well at detecting small numbers of synthetic lethal genes in simple systems. It does not perform as well in more complex systems but neither do alternative strategies. The SLIPT methodology performs well compared to Pearson correlation and similar methods based on the χ^2 test. Thus SLIPT is an effective detection method for synthetic lethal relationships in expression data despite its relatively simple design.

Simulations of more complex datasets, including large numbers of genes, complex correlation structure derived from graph structures, and correlations with the query gene. SLIPT performs robustly across these, including correlation structures based on complex biological pathways. The performance of SLIPT improves in larger datasets,

datasets with positive correlations with the query genes, and some graph structures which include inhibiting relationships, namely those datasets more representative of gene expression in biological data. SLIPT was both capable of recurrently detecting genes within a synthetic lethal pathway and distinguishing synthetic lethal genes from correlated with them, even in highly complex correlation structures. Therefore SLIPT is a stringent synthetic lethal detection strategy and is applicable to gene expression as previously demonstrated for the partners of *CDH1* in breast and stomach cancer in this thesis.

References

Aarts, M., Bajrami, I., Herrera-Abreu, M.T., Elliott, R., Brough, R., Ashworth, A., Lord, C.J., and Turner, N.C. (2015) Functional genetic screen identifies increased sensitivity to wee1 inhibition in cells with defects in fanconi anemia and hr pathways. *Mol Cancer Ther*, **14**(4): 865–76.

Adler, D. (2005) *vioplot: Violin plot.* R package version 0.2.

Akobeng, A.K. (2007) Understanding diagnostic tests 3: receiver operating characteristic curves. *Acta Pdiatrica*, **96**(5): 644–647.

American Cancer Society (2017) Genetics and cancer. `https://www.cancer.org/cancer/cancer-causes/genetics.html`. Accessed: 22/03/2017.

Anjomshoaa, A., Lin, Y.H., Black, M.A., McCall, J.L., Humar, B., Song, S., Fukuzawa, R., Yoon, H.S., Holzmann, B., Friederichs, J., *et al.* (2008) Reduced expression of a gene proliferation signature is associated with enhanced malignancy in colon cancer. *Br J Cancer*, **99**(6): 966–973.

Araki, H., Knapp, C., Tsai, P., and Print, C. (2012) GeneSetDB: A comprehensive meta-database, statistical and visualisation framework for gene set analysis. *FEBS Open Bio*, **2**: 76–82.

Ashburner, M., Ball, C.A., Blake, J.A., Botstein, D., Butler, H., Cherry, J.M., Davis, A.P., Dolinski, K., Dwight, S.S., Eppig, J.T., *et al.* (2000) Gene ontology: tool for the unification of biology. The Gene Ontology Consortium. *Nat Genet*, **25**(1): 25–29.

Ashworth, A. (2008) A synthetic lethal therapeutic approach: poly(adp) ribose polymerase inhibitors for the treatment of cancers deficient in dna double-strand break repair. *J Clin Oncol*, **26**(22): 3785–90.

Audeh, M.W., Carmichael, J., Penson, R.T., Friedlander, M., Powell, B., Bell-McGuinn, K.M., Scott, C., Weitzel, J.N., Oaknin, A., Loman, N., *et al.* (2010) Oral

poly(adp-ribose) polymerase inhibitor olaparib in patients with *BRCA1* or *BRCA2* mutations and recurrent ovarian cancer: a proof-of-concept trial. *Lancet*, **376**(9737): 245–51.

Babyak, M.A. (2004) What you see may not be what you get: a brief, nontechnical introduction to overfitting in regression-type models. *Psychosom Med*, **66**(3): 411–21.

Bamford, S., Dawson, E., Forbes, S., Clements, J., Pettett, R., Dogan, A., Flanagan, A., Teague, J., Futreal, P.A., Stratton, M.R., *et al.* (2004) The COSMIC (Catalogue of Somatic Mutations in Cancer) database and website. *Br J Cancer*, **91**(2): 355–358.

Barabási, A.L. and Albert, R. (1999) Emergence of scaling in random networks. *Science*, **286**(5439): 509–12.

Barabási, A.L., Gulbahce, N., and Loscalzo, J. (2011) Network medicine: a network-based approach to human disease. *Nat Rev Genet*, **12**(1): 56–68.

Barabási, A.L. and Oltvai, Z.N. (2004) Network biology: understanding the cell's functional organization. *Nat Rev Genet*, **5**(2): 101–13.

Barrat, A. and Weigt, M. (2000) On the properties of small-world network models. *The European Physical Journal B - Condensed Matter and Complex Systems*, **13**(3): 547–560.

Barretina, J., Caponigro, G., Stransky, N., Venkatesan, K., Margolin, A.A., Kim, S., Wilson, C.J., Lehar, J., Kryukov, G.V., Sonkin, D., *et al.* (2012) The Cancer Cell Line Encyclopedia enables predictive modelling of anticancer drug sensitivity. *Nature*, **483**(7391): 603–607.

Barry, W.T. (2016) *safe: Significance Analysis of Function and Expression*. R package version 3.14.0.

Baryshnikova, A., Costanzo, M., Dixon, S., Vizeacoumar, F.J., Myers, C.L., Andrews, B., and Boone, C. (2010a) Synthetic genetic array (sga) analysis in saccharomyces cerevisiae and schizosaccharomyces pombe. *Methods Enzymol*, **470**: 145–79.

Baryshnikova, A., Costanzo, M., Kim, Y., Ding, H., Koh, J., Toufighi, K., Youn, J.Y., Ou, J., San Luis, B.J., Bandyopadhyay, S., *et al.* (2010b) Quantitative analysis of

fitness and genetic interactions in yeast on a genome scale. *Nat Meth*, **7**(12): 1017–1024.

Bass, A.J., Thorsson, V., Shmulevich, I., Reynolds, S.M., Miller, M., Bernard, B., Hinoue, T., Laird, P.W., Curtis, C., Shen, H., *et al.* (2014) Comprehensive molecular characterization of gastric adenocarcinoma. *Nature*, **513**(7517): 202–209.

Bates, D. and Maechler, M. (2016) *Matrix: Sparse and Dense Matrix Classes and Methods*. R package version 1.2-7.1.

Bateson, W. and Mendel, G. (1909) *Mendel's principles of heredity, by W. Bateson*. University Press, Cambridge [Eng.].

Becker, K.F., Atkinson, M.J., Reich, U., Becker, I., Nekarda, H., Siewert, J.R., and Hfler, H. (1994) E-cadherin gene mutations provide clues to diffuse type gastric carcinomas. *Cancer Research*, **54**(14): 3845–3852.

Bell, D., Berchuck, A., Birrer, M., Chien, J., Cramer, D., Dao, F., Dhir, R., DiSaia, P., Gabra, H., Glenn, P., *et al.* (2011) Integrated genomic analyses of ovarian carcinoma. *Nature*, **474**(7353): 609–615.

Benjamini, Y. and Hochberg, Y. (1995) Controlling the false discovery rate: A practical and powerful approach to multiple testing. *Journal of the Royal Statistical Society Series B (Methodological)*, **57**(1): 289–300.

Berx, G., Cleton-Jansen, A.M., Nollet, F., de Leeuw, W.J., van de Vijver, M., Cornelisse, C., and van Roy, F. (1995) E-cadherin is a tumour/invasion suppressor gene mutated in human lobular breast cancers. *EMBO J*, **14**(24): 6107–15.

Berx, G., Cleton-Jansen, A.M., Strumane, K., de Leeuw, W.J., Nollet, F., van Roy, F., and Cornelisse, C. (1996) E-cadherin is inactivated in a majority of invasive human lobular breast cancers by truncation mutations throughout its extracellular domain. *Oncogene*, **13**(9): 1919–25.

Berx, G. and van Roy, F. (2009) Involvement of members of the cadherin superfamily in cancer. *Cold Spring Harb Perspect Biol*, **1**: a003129.

Bitler, B.G., Aird, K.M., Garipov, A., Li, H., Amatangelo, M., Kossenkov, A.V., Schultz, D.C., Liu, Q., Shih Ie, M., Conejo-Garcia, J.R., *et al.* (2015) Synthetic lethality by targeting ezh2 methyltransferase activity in arid1a-mutated cancers. *Nat Med*, **21**(3): 231–8.

Blake, J.A., Christie, K.R., Dolan, M.E., Drabkin, H.J., Hill, D.P., Ni, L., Sitnikov, D., Burgess, S., Buza, T., Gresham, C., *et al.* (2015) Gene Ontology Consortium: going forward. *Nucleic Acids Res*, **43**(Database issue): D1049–1056.

Boettcher, M., Lawson, A., Ladenburger, V., Fredebohm, J., Wolf, J., Hoheisel, J.D., Frezza, C., and Shlomi, T. (2014) High throughput synthetic lethality screen reveals a tumorigenic role of adenylate cyclase in fumarate hydratase-deficient cancer cells. *BMC Genomics*, **15**: 158.

Boone, C., Bussey, H., and Andrews, B.J. (2007) Exploring genetic interactions and networks with yeast. *Nat Rev Genet*, **8**(6): 437–49.

Borgatti, S.P. (2005) Centrality and network flow. *Social Networks*, **27**(1): 55 – 71.

Boucher, B. and Jenna, S. (2013) Genetic interaction networks: better understand to better predict. *Front Genet*, **4**: 290.

Bozovic-Spasojevic, I., Azambuja, E., McCaskill-Stevens, W., Dinh, P., and Cardoso, F. (2012) Chemoprevention for breast cancer. *Cancer treatment reviews*, **38**(5): 329–339.

Breiman, L. (2001) Random forests. *Machine Learning*, **45**(1): 5–32.

Brin, S. and Page, L. (1998) The anatomy of a large-scale hypertextual web search engine. *Computer Networks and ISDN Systems*, **30**(1): 107 – 117.

Brouxhon, S.M., Kyrkanides, S., Teng, X., Athar, M., Ghazizadeh, S., Simon, M., O'Banion, M.K., and Ma, L. (2014) Soluble E-cadherin: a critical oncogene modulating receptor tyrosine kinases, MAPK and PI3K/Akt/mTOR signaling. *Oncogene*, **33**(2): 225–235.

Bryant, H.E., Schultz, N., Thomas, H.D., Parker, K.M., Flower, D., Lopez, E., Kyle, S., Meuth, M., Curtin, N.J., and Helleday, T. (2005) Specific killing of *BRCA2*-deficient tumours with inhibitors of poly*adpribose* polymerase. *Nature*, **434**(7035): 913–7.

Bussey, H., Andrews, B., and Boone, C. (2006) From worm genetic networks to complex human diseases. *Nat Genet*, **38**(8): 862–3.

Butland, G., Babu, M., Diaz-Mejia, J.J., Bohdana, F., Phanse, S., Gold, B., Yang, W., Li, J., Gagarinova, A.G., Pogoutse, O., *et al.* (2008) esga: E. coli synthetic genetic array analysis. *Nat Methods*, **5**(9): 789–95.

cBioPortal for Cancer Genomics (cBioPortal) (2017) cBioPortal for Cancer Genomics. `http://www.cbioportal.org/`. Accessed: 26/03/2017.

Cerami, E.G., Gross, B.E., Demir, E., Rodchenkov, I., Babur, O., Anwar, N., Schultz, N., Bader, G.D., and Sander, C. (2011) Pathway Commons, a web resource for biological pathway data. *Nucleic Acids Res*, **39**(Database issue): D685–690.

Chen, A., Beetham, H., Black, M.A., Priya, R., Telford, B.J., Guest, J., Wiggins, G.A.R., Godwin, T.D., Yap, A.S., and Guilford, P.J. (2014) E-cadherin loss alters cytoskeletal organization and adhesion in non-malignant breast cells but is insufficient to induce an epithelial-mesenchymal transition. *BMC Cancer*, **14**(1): 552.

Chen, S. and Parmigiani, G. (2007) Meta-analysis of BRCA1 and BRCA2 penetrance. *J Clin Oncol*, **25**(11): 1329–1333.

Chen, X. and Tompa, M. (2010) Comparative assessment of methods for aligning multiple genome sequences. *Nat Biotechnol*, **28**(6): 567–572.

Chipman, K. and Singh, A. (2009) Predicting genetic interactions with random walks on biological networks. *BMC Bioinformatics*, **10**(1): 17.

Christofori, G. and Semb, H. (1999) The role of the cell-adhesion molecule E-cadherin as a tumour-suppressor gene. *Trends in Biochemical Sciences*, **24**(2): 73 – 76.

Ciriello, G., Gatza, M.L., Beck, A.H., Wilkerson, M.D., Rhie, S.K., Pastore, A., Zhang, H., McLellan, M., Yau, C., Kandoth, C., *et al.* (2015) Comprehensive Molecular Portraits of Invasive Lobular Breast Cancer. *Cell*, **163**(2): 506–519.

Clark, M.J. (2004) Endogenous Regulator of G Protein Signaling Proteins Suppress G o-Dependent -Opioid Agonist-Mediated Adenylyl Cyclase Supersensitization. *Journal of Pharmacology and Experimental Therapeutics*, **310**(1): 215–222.

Clough, E. and Barrett, T. (2016) The Gene Expression Omnibus Database. *Methods Mol Biol*, **1418**: 93–110.

Collingridge, D.S. (2013) A primer on quantitized data analysis and permutation testing. *Journal of Mixed Methods Research*, **7**(1): 81–97.

Collins, F.S. and Barker, A.D. (2007) Mapping the cancer genome. Pinpointing the genes involved in cancer will help chart a new course across the complex landscape of human malignancies. *Sci Am*, **296**(3): 50–57.

Collisson, E., Campbell, J., Brooks, A., Berger, A., Lee, W., Chmielecki, J., Beer, D., Cope, L., Creighton, C., Danilova, L., *et al.* (2014) Comprehensive molecular profiling of lung adenocarcinoma. *Nature*, **511**(7511): 543–550.

Corcoran, R.B., Ebi, H., Turke, A.B., Coffee, E.M., Nishino, M., Cogdill, A.P., Brown, R.D., Della Pelle, P., Dias-Santagata, D., Hung, K.E., *et al.* (2012) Egfr-mediated re-activation of mapk signaling contributes to insensitivity of *BRAF*-mutant colorectal cancers to raf inhibition with vemurafenib. *Cancer Discovery*, **2**(3): 227–235.

Costanzo, M., Baryshnikova, A., Bellay, J., Kim, Y., Spear, E.D., Sevier, C.S., Ding, H., Koh, J.L., Toufighi, K., Mostafavi, S., *et al.* (2010) The genetic landscape of a cell. *Science*, **327**(5964): 425–31.

Costanzo, M., Baryshnikova, A., Myers, C.L., Andrews, B., and Boone, C. (2011) Charting the genetic interaction map of a cell. *Curr Opin Biotechnol*, **22**(1): 66–74.

Courtney, K.D., Corcoran, R.B., and Engelman, J.A. (2010) The PI3K pathway as drug target in human cancer. *J Clin Oncol*, **28**(6): 1075–1083.

Croft, D., Mundo, A.F., Haw, R., Milacic, M., Weiser, J., Wu, G., Caudy, M., Garapati, P., Gillespie, M., Kamdar, M.R., *et al.* (2014) The Reactome pathway knowledgebase. *Nucleic Acids Res*, **42**(database issue): D472D477.

Crunkhorn, S. (2014) Cancer: Predicting synthetic lethal interactions. *Nat Rev Drug Discov*, **13**(11): 812.

Csardi, G. and Nepusz, T. (2006) The igraph software package for complex network research. *InterJournal*, **Complex Systems**: 1695.

Dai, X., Li, T., Bai, Z., Yang, Y., Liu, X., Zhan, J., and Shi, B. (2015) Breast cancer intrinsic subtype classification, clinical use and future trends. *Am J Cancer Res*, **5**(10): 2929–2943.

Davierwala, A.P., Haynes, J., Li, Z., Brost, R.L., Robinson, M.D., Yu, L., Mnaimneh, S., Ding, H., Zhu, H., Chen, Y., *et al.* (2005) The synthetic genetic interaction spectrum of essential genes. *Nat Genet*, **37**(10): 1147–1152.

De Leeuw, W.J., Berx, G., Vos, C.B., Peterse, J.L., Van de Vijver, M.J., Litvinov, S., Van Roy, F., Cornelisse, C.J., and Cleton-Jansen, A.M. (1997) Simultaneous loss of E-cadherin and catenins in invasive lobular breast cancer and lobular carcinoma in situ. *J Pathol*, **183**(4): 404–11.

De Santis, G., Miotti, S., Mazzi, M., Canevari, S., and Tomassetti, A. (2009) E-cadherin directly contributes to PI3K/AKT activation by engaging the PI3K-p85 regulatory subunit to adherens junctions of ovarian carcinoma cells. *Oncogene*, **28**(9): 1206–1217.

Demir, E., Babur, O., Rodchenkov, I., Aksoy, B.A., Fukuda, K.I., Gross, B., Sumer, O.S., Bader, G.D., and Sander, C. (2013) Using biological pathway data with Paxtools. *PLoS Comput Biol*, **9**(9): e1003194.

Deshpande, R., Asiedu, M.K., Klebig, M., Sutor, S., Kuzmin, E., Nelson, J., Piotrowski, J., Shin, S.H., Yoshida, M., Costanzo, M., *et al.* (2013) A comparative genomic approach for identifying synthetic lethal interactions in human cancer. *Cancer Res*, **73**(20): 6128–36.

Dickson, D. (1999) Wellcome funds cancer database. *Nature*, **401**(6755): 729.

Dienstmann, R. and Tabernero, J. (2011) *BRAF* as a target for cancer therapy. *Anticancer Agents Med Chem*, **11**(3): 285–95.

Dijkstra, E.W. (1959) A note on two problems in connexion with graphs. *Numerische Mathematik*, **1**(1): 269–271.

Dixon, S.J., Andrews, B.J., and Boone, C. (2009) Exploring the conservation of synthetic lethal genetic interaction networks. *Commun Integr Biol*, **2**(2): 78–81.

Dixon, S.J., Fedyshyn, Y., Koh, J.L., Prasad, T.S., Chahwan, C., Chua, G., Toufighi, K., Baryshnikova, A., Hayles, J., Hoe, K.L., *et al.* (2008) Significant conservation of synthetic lethal genetic interaction networks between distantly related eukaryotes. *Proc Natl Acad Sci U S A*, **105**(43): 16653–8.

Dong, L.L., Liu, L., Ma, C.H., Li, J.S., Du, C., Xu, S., Han, L.H., Li, L., and Wang, X.W. (2012) E-cadherin promotes proliferation of human ovarian cancer cells in vitro via activating MEK/ERK pathway. *Acta Pharmacol Sin*, **33**(6): 817–822.

Dorogovtsev, S.N. and Mendes, J.F. (2003) *Evolution of networks: From biological nets to the Internet and WWW*. Oxford University Press, USA.

Dorsam, R.T. and Gutkind, J.S. (2007) G-protein-coupled receptors and cancer. *Nat Rev Cancer*, **7**(2): 79–94.

Erdős, P. and Rényi, A. (1959) On random graphs I. *Publ Math Debrecen*, **6**: 290–297.

Erdős, P. and Rényi, A. (1960) On the evolution of random graphs. In *Publ. Math. Inst. Hung. Acad. Sci*, volume 5, 17–61.

Eroles, P., Bosch, A., Perez-Fidalgo, J.A., and Lluch, A. (2012) Molecular biology in breast cancer: intrinsic subtypes and signaling pathways. *Cancer Treat Rev*, **38**(6): 698–707.

Farmer, H., McCabe, N., Lord, C.J., Tutt, A.N., Johnson, D.A., Richardson, T.B., Santarosa, M., Dillon, K.J., Hickson, I., Knights, C., *et al.* (2005) Targeting the dna repair defect in BRCA mutant cells as a therapeutic strategy. *Nature*, **434**(7035): 917–21.

Fawcett, T. (2006) An introduction to ROC analysis. *Pattern Recognition Letters*, **27**(8): 861 – 874. {ROC} Analysis in Pattern Recognition.

Fece de la Cruz, F., Gapp, B.V., and Nijman, S.M. (2015) Synthetic lethal vulnerabilities of cancer. *Annu Rev Pharmacol Toxicol*, **55**: 513–531.

Ferlay, J., Soerjomataram, I., Dikshit, R., Eser, S., Mathers, C., Rebelo, M., Parkin, D.M., Forman, D., and Bray, F. (2015) Cancer incidence and mortality worldwide: sources, methods and major patterns in GLOBOCAN 2012. *Int J Cancer*, **136**(5): E359–386.

Fisher, R.A. (1919) Xv.the correlation between relatives on the supposition of mendelian inheritance. *Earth and Environmental Science Transactions of the Royal Society of Edinburgh*, **52**(02): 399–433.

Fong, P.C., Boss, D.S., Yap, T.A., Tutt, A., Wu, P., Mergui-Roelvink, M., Mortimer, P., Swaisland, H., Lau, A., O'Connor, M.J., *et al.* (2009) Inhibition of poly(adp-ribose) polymerase in tumors from BRCA mutation carriers. *N Engl J Med*, **361**(2): 123–34.

Fong, P.C., Yap, T.A., Boss, D.S., Carden, C.P., Mergui-Roelvink, M., Gourley, C., De Greve, J., Lubinski, J., Shanley, S., Messiou, C., *et al.* (2010) Poly(adp)-ribose polymerase inhibition: frequent durable responses in BRCA carrier ovarian cancer correlating with platinum-free interval. *J Clin Oncol*, **28**(15): 2512–9.

Forbes, S.A., Beare, D., Gunasekaran, P., Leung, K., Bindal, N., Boutselakis, H., Ding, M., Bamford, S., Cole, C., Ward, S., *et al.* (2015) COSMIC: exploring the world's knowledge of somatic mutations in human cancer. *Nucleic Acids Res*, **43**(Database issue): D805–811.

Fraser, A. (2004) Towards full employment: using RNAi to find roles for the redundant. *Oncogene*, **23**(51): 8346–52.

Futreal, P.A., Coin, L., Marshall, M., Down, T., Hubbard, T., Wooster, R., Rahman, N., and Stratton, M.R. (2004) A census of human cancer genes. *Nat Rev Cancer*, **4**(3): 177–183.

Futreal, P.A., Kasprzyk, A., Birney, E., Mullikin, J.C., Wooster, R., and Stratton, M.R. (2001) Cancer and genomics. *Nature*, **409**(6822): 850–852.

Gao, B. and Roux, P.P. (2015) Translational control by oncogenic signaling pathways. *Biochimica et Biophysica Acta*, **1849**(7): 753–65.

Gatza, M.L., Kung, H.N., Blackwell, K.L., Dewhirst, M.W., Marks, J.R., and Chi, J.T. (2011) Analysis of tumor environmental response and oncogenic pathway activation identifies distinct basal and luminal features in HER2-related breast tumor subtypes. *Breast Cancer Res*, **13**(3): R62.

Gatza, M.L., Lucas, J.E., Barry, W.T., Kim, J.W., Wang, Q., Crawford, M.D., Datto, M.B., Kelley, M., Mathey-Prevot, B., Potti, A., *et al.* (2010) A pathway-based classification of human breast cancer. *Proc Natl Acad Sci USA*, **107**(15): 6994–6999.

Gatza, M.L., Silva, G.O., Parker, J.S., Fan, C., and Perou, C.M. (2014) An integrated genomics approach identifies drivers of proliferation in luminal-subtype human breast cancer. *Nat Genet*, **46**(10): 1051–1059.

Gentleman, R.C., Carey, V.J., Bates, D.M., Bolstad, B., Dettling, M., Dudoit, S., Ellis, B., Gautier, L., Ge, Y., Gentry, J., *et al.* (2004) Bioconductor: open software development for computational biology and bioinformatics. *Genome Biol*, **5**(10): R80.

Genz, A. and Bretz, F. (2009) Computation of multivariate normal and t probabilities. In *Lecture Notes in Statistics*, volume 195. Springer-Verlag, Heidelberg.

Genz, A., Bretz, F., Miwa, T., Mi, X., Leisch, F., Scheipl, F., and Hothorn, T. (2016) *mvtnorm: Multivariate Normal and t Distributions*. R package version 1.0-5. URL.

Glaire, M.A., Brown, M., Church, D.N., and Tomlinson, I. (2017) Cancer predisposition syndromes: lessons for truly precision medicine. *J Pathol*, **241**(2): 226–235.

Globus (Globus) (2017) Research data management simplified. `https://www.globus.org/`. Accessed: 25/03/2017.

Goodwin, S., McPherson, J.D., and McCombie, W.R. (2016) Coming of age: ten years of next-generation sequencing technologies. *Nat Rev Genet*, **17**(6): 333–351.

Grady, W.M., Willis, J., Guilford, P.J., Dunbier, A.K., Toro, T.T., Lynch, H., Wiesner, G., Ferguson, K., Eng, C., Park, J.G., *et al.* (2000) Methylation of the CDH1 promoter as the second genetic hit in hereditary diffuse gastric cancer. *Nat Genet*, **26**(1): 16–17.

Graziano, F., Humar, B., and Guilford, P. (2003) The role of the E-cadherin gene (*CDH1*) in diffuse gastric cancer susceptibility: from the laboratory to clinical practice. *Annals of Oncology*, **14**(12): 1705–1713.

Güell, O., Sagus, F., and Serrano, M. (2014) Essential plasticity and redundancy of metabolism unveiled by synthetic lethality analysis. *PLoS Comput Biol*, **10**(5): e1003637.

Guilford, P. (1999) E-cadherin downregulation in cancer: fuel on the fire? *Molecular Medicine Today*, **5**(4): 172 – 177.

Guilford, P., Hopkins, J., Harraway, J., McLeod, M., McLeod, N., Harawira, P., Taite, H., Scoular, R., Miller, A., and Reeve, A.E. (1998) E-cadherin germline mutations in familial gastric cancer. *Nature*, **392**(6674): 402–5.

Guilford, P., Humar, B., and Blair, V. (2010) Hereditary diffuse gastric cancer: translation of *CDH1* germline mutations into clinical practice. *Gastric Cancer*, **13**(1): 1–10.

Guilford, P.J., Hopkins, J.B., Grady, W.M., Markowitz, S.D., Willis, J., Lynch, H., Rajput, A., Wiesner, G.L., Lindor, N.M., Burgart, L.J., *et al.* (1999) E-cadherin germline mutations define an inherited cancer syndrome dominated by diffuse gastric cancer. *Hum Mutat*, **14**(3): 249–55.

Guo, J., Liu, H., and Zheng, J. (2016) SynLethDB: synthetic lethality database toward discovery of selective and sensitive anticancer drug targets. *Nucleic Acids Res*, **44**(D1): D1011–1017.

Hajian-Tilaki, K. (2013) Receiver Operating Characteristic (ROC) Curve Analysis for Medical Diagnostic Test Evaluation. *Caspian J Intern Med*, **4**(2): 627–635.

Hall, M., Frank, E., Holmes, G., Pfahringer, B., Reutemann, P., and Witten, I.H. (2009) The weka data mining software: an update. *SIGKDD Explor Newsl*, **11**(1): 10–18.

Hammerman, P.S., Lawrence, M.S., Voet, D., Jing, R., Cibulskis, K., Sivachenko, A., Stojanov, P., McKenna, A., Lander, E.S., Gabriel, S., *et al.* (2012) Comprehensive genomic characterization of squamous cell lung cancers. *Nature*, **489**(7417): 519–525.

Hanahan, D. and Weinberg, R.A. (2000) The hallmarks of cancer. *Cell*, **100**(1): 57–70.

Hanahan, D. and Weinberg, R.A. (2011) Hallmarks of cancer: the next generation. *Cell*, **144**(5): 646–674.

Hanna, S. (2003) Cancer incidence in new zealand (2003-2007). In D. Forman, D. Bray F Brewster, C. Gombe Mbalawa, B. Kohler, M. Piñeros, E. Steliarova-Foucher, R. Swaminathan, and J. Ferlay (editors), *Cancer Incidence in Five Continents*, volume X, 902–907. International Agency for Research on Cancer, Lyon, France. Electronic version `http://ci5.iarc.fr` Accessed 22/03/2017.

Hansford, S., Kaurah, P., Li-Chang, H., Woo, M., Senz, J., Pinheiro, H., Schrader, K.A., Schaeffer, D.F., Shumansky, K., Zogopoulos, G., *et al.* (2015) Hereditary Diffuse Gastric Cancer Syndrome: CDH1 Mutations and Beyond. *JAMA Oncol*, **1**(1): 23–32.

Heiskanen, M., Bian, X., Swan, D., and Basu, A. (2014) caArray microarray database in the cancer biomedical informatics grid$^{\text{TM}}$ (caBIG$^{\text{TM}}$). *Cancer Research*, **67**(9 Supplement): 3712–3712.

Heiskanen, M.A. and Aittokallio, T. (2012) Mining high-throughput screens for cancer drug targets-lessons from yeast chemical-genomic profiling and synthetic lethality. *Wiley Interdisciplinary Reviews: Data Mining and Knowledge Discovery*, **2**(3): 263–272.

Hell, P. (1976) Graphs with given neighbourhoods i. problémes combinatorics at theorie des graphes. *Proc Coil Int CNRS, Orsay*, **260**: 219–223.

Hillenmeyer, M.E. (2008) The chemical genomic portrait of yeast: uncovering a phenotype for all genes. *Science*, **320**: 362–365.

Hoadley, K.A., Yau, C., Wolf, D.M., Cherniack, A.D., Tamborero, D., Ng, S., Leiserson, M.D., Niu, B., McLellan, M.D., Uzunangelov, V., *et al.* (2014) Multiplatform analysis of 12 cancer types reveals molecular classification within and across tissues of origin. *Cell*, **158**(4): 929–944.

Hoehndorf, R., Hardy, N.W., Osumi-Sutherland, D., Tweedie, S., Schofield, P.N., and Gkoutos, G.V. (2013) Systematic analysis of experimental phenotype data reveals gene functions. *PLoS ONE*, **8**(4): e60847.

Holm, S. (1979) A simple sequentially rejective multiple test procedure. *Scandinavian Journal of Statistics*, **6**(2): 65–70.

Holme, P. and Kim, B.J. (2002) Growing scale-free networks with tunable clustering. *Physical Review E*, **65**(2): 026107.

Hopkins, A.L. (2008) Network pharmacology: the next paradigm in drug discovery. *Nat Chem Biol*, **4**(11): 682–690.

Hu, Z., Fan, C., Oh, D.S., Marron, J.S., He, X., Qaqish, B.F., Livasy, C., Carey, L.A., Reynolds, E., Dressler, L., *et al.* (2006) The molecular portraits of breast tumors are conserved across microarray platforms. *BMC Genomics*, **7**: 96.

Huang, E., Cheng, S., Dressman, H., Pittman, J., Tsou, M., Horng, C., Bild, A., Iversen, E., Liao, M., Chen, C., *et al.* (2003) Gene expression predictors of breast cancer outcomes. *Lancet*, **361**: 1590–1596.

International HapMap 3 Consortium (HapMap) (2003) The International HapMap Project. *Nature*, **426**(6968): 789–796.

Jeanes, A., Gottardi, C.J., and Yap, A.S. (2008) Cadherins and cancer: how does cadherin dysfunction promote tumor progression? *Oncogene*, **27**(55): 6920–6929.

Jerby-Arnon, L., Pfetzer, N., Waldman, Y., McGarry, L., James, D., Shanks, E., Seashore-Ludlow, B., Weinstock, A., Geiger, T., Clemons, P., *et al.* (2014) Predicting cancer-specific vulnerability via data-driven detection of synthetic lethality. *Cell*, **158**(5): 1199–1209.

Joachims, T. (1999) Making large-scale support vector machine learning practical. In S. Bernhard, lkopf, J.C.B. Christopher, and J.S. Alexander (editors), *Advances in kernel methods*, 169–184. MIT Press.

Ju, Z., Liu, W., Roebuck, P.L., Siwak, D.R., Zhang, N., Lu, Y., Davies, M.A., Akbani, R., Weinstein, J.N., Mills, G.B., *et al.* (2015) Development of a robust classifier for quality control of reverse-phase protein arrays. *Bioinformatics*, **31**(6): 912.

Kaelin, Jr, W. (2005) The concept of synthetic lethality in the context of anticancer therapy. *Nat Rev Cancer*, **5**(9): 689–98.

Kaelin, Jr, W. (2009) Synthetic lethality: a framework for the development of wiser cancer therapeutics. *Genome Med*, **1**: 99.

Kamada, T. and Kawai, S. (1989) An algorithm for drawing general undirected graphs. *Information Processing Letters*, **31**(1): 7–15.

Kelley, R. and Ideker, T. (2005) Systematic interpretation of genetic interactions using protein networks. *Nat Biotech*, **23**(5): 561–566.

Kelly, S.T. (2013) *Statistical Predictions of Synthetic Lethal Interactions in Cancer*. Dissertation, University of Otago.

Kelly, S.T., Single, A.B., Telford, B.J., Beetham, H.G., Godwin, T.D., Chen, A., Black, M.A., and Guilford, P.J. (unpublished) Towards HDGC chemoprevention: vulnerabilities in E-cadherin-negative cells identified by genome-wide interrogation of isogenic cell lines and whole tumors. Submitted to *Cancer Prev Res*.

Kim, N.G., Koh, E., Chen, X., and Gumbiner, B.M. (2011) E-cadherin mediates contact inhibition of proliferation through Hippo signaling-pathway components. *Proc Natl Acad Sci USA*, **108**(29): 11930–11935.

Kozlov, K.N., Gursky, V.V., Kulakovskiy, I.V., and Samsonova, M.G. (2015) Sequence-based model of gap gene regulation network. *BMC Genomics*, **15**(Suppl 12): S6.

Kranthi, S., Rao, S., and Manimaran, P. (2013) Identification of synthetic lethal pairs in biological systems through network information centrality. *Mol BioSyst*, **9**(8): 2163–2167.

Kroepil, F., Fluegen, G., Totikov, Z., Baldus, S.E., Vay, C., Schauer, M., Topp, S.A., Esch, J.S., Knoefel, W.T., and Stoecklein, N.H. (2012) Down-regulation of CDH1

is associated with expression of SNAI1 in colorectal adenomas. *PLoS ONE*, **7**(9): e46665.

Lander, E.S. (2011) Initial impact of the sequencing of the human genome. *Nature*, **470**(7333): 187–197.

Lander, E.S., Linton, L.M., Birren, B., Nusbaum, C., Zody, M.C., Baldwin, J., Devon, K., Dewar, K., Doyle, M., FitzHugh, W., *et al.* (2001) Initial sequencing and analysis of the human genome. *Nature*, **409**(6822): 860–921.

Langmead, B., Trapnell, C., Pop, M., and Salzberg, S.L. (2009) Ultrafast and memory-efficient alignment of short DNA sequences to the human genome. *Genome Biol*, **10**(3): R25.

Latora, V. and Marchiori, M. (2001) Efficient behavior of small-world networks. *Phys Rev Lett*, **87**: 198701.

Laufer, C., Fischer, B., Billmann, M., Huber, W., and Boutros, M. (2013) Mapping genetic interactions in human cancer cells with RNAi and multiparametric phenotyping. *Nat Methods*, **10**(5): 427–31.

Law, C.W., Chen, Y., Shi, W., and Smyth, G.K. (2014) voom: precision weights unlock linear model analysis tools for RNA-seq read counts. *Genome Biol*, **15**(2): R29.

Le Meur, N. and Gentleman, R. (2008) Modeling synthetic lethality. *Genome Biol*, **9**(9): R135.

Le Meur, N., Jiang, Z., Liu, T., Mar, J., and Gentleman, R.C. (2014) Slgi: Synthetic lethal genetic interaction. r package version 1.26.0.

Lee, A.Y., Perreault, R., Harel, S., Boulier, E.L., Suderman, M., Hallett, M., and Jenna, S. (2010a) Searching for signaling balance through the identification of genetic interactors of the rab guanine-nucleotide dissociation inhibitor gdi-1. *PLoS ONE*, **5**(5): e10624.

Lee, I., Lehner, B., Vavouri, T., Shin, J., Fraser, A.G., and Marcotte, E.M. (2010b) Predicting genetic modifier loci using functional gene networks. *Genome Research*, **20**(8): 1143–1153.

Lee, I. and Marcotte, E.M. (2009) Effects of functional bias on supervised learning of a gene network model. *Methods Mol Biol*, **541**: 463–75.

Lee, M.J., Ye, A.S., Gardino, A.K., Heijink, A.M., Sorger, P.K., MacBeath, G., and Yaffe, M.B. (2012) Sequential application of anticancer drugs enhances cell death by rewiring apoptotic signaling networks. *Cell*, **149**(4): 780–94.

Lehner, B., Crombie, C., Tischler, J., Fortunato, A., and Fraser, A.G. (2006) Systematic mapping of genetic interactions in caenorhabditis elegans identifies common modifiers of diverse signaling pathways. *Nat Genet*, **38**(8): 896–903.

Li, X.J., Mishra, S.K., Wu, M., Zhang, F., and Zheng, J. (2014) Syn-lethality: An integrative knowledge base of synthetic lethality towards discovery of selective anticancer therapies. *Biomed Res Int*, **2014**: 196034.

Lokody, I. (2014) Computational modelling: A computational crystal ball. *Nature Reviews Cancer*, **14**(10): 649–649.

Lord, C.J., Tutt, A.N., and Ashworth, A. (2015) Synthetic lethality and cancer therapy: lessons learned from the development of PARP inhibitors. *Annu Rev Med*, **66**: 455–470.

Lu, X., Kensche, P.R., Huynen, M.A., and Notebaart, R.A. (2013) Genome evolution predicts genetic interactions in protein complexes and reveals cancer drug targets. *Nat Commun*, **4**: 2124.

Lu, X., Megchelenbrink, W., Notebaart, R.A., and Huynen, M.A. (2015) Predicting human genetic interactions from cancer genome evolution. *PLoS One*, **10**(5): e0125795.

Lum, P.Y., Armour, C.D., Stepaniants, S.B., Cavet, G., Wolf, M.K., Butler, J.S., Hinshaw, J.C., Garnier, P., Prestwich, G.D., Leonardson, A., *et al.* (2004) Discovering modes of action for therapeutic compounds using a genome-wide screen of yeast heterozygotes. *Cell*, **116**(1): 121–137.

Luo, J., Solimini, N.L., and Elledge, S.J. (2009) Principles of Cancer Therapy: Oncogene and Non-oncogene Addiction. *Cell*, **136**(5): 823–837.

Machado, J., Olivera, C., Carvalh, R., Soares, P., Berx, G., Caldas, C., Sercuca, R., Carneiro, F., and Sorbrinho-Simoes, M. (2001) E-cadherin gene (*CDH1*) promoter methylation as the second hit in sporadic diffuse gastric carcinoma. *Oncogene*, **20**: 1525–1528.

Markowetz, F. (2017) All biology is computational biology. *PLoS Biol*, **15**(3): e2002050.

Masciari, S., Larsson, N., Senz, J., Boyd, N., Kaurah, P., Kandel, M.J., Harris, L.N., Pinheiro, H.C., Troussard, A., Miron, P., *et al.* (2007) Germline E-cadherin mutations in familial lobular breast cancer. *J Med Genet*, **44**(11): 726–31.

Mattison, J., van der Weyden, L., Hubbard, T., and Adams, D.J. (2009) Cancer gene discovery in mouse and man. *Biochim Biophys Acta*, **1796**(2): 140–161.

McLachlan, J., George, A., and Banerjee, S. (2016) The current status of parp inhibitors in ovarian cancer. *Tumori*, **102**(5): 433–440.

McLendon, R., Friedman, A., Bigner, D., Van Meir, E.G., Brat, D.J., Mastrogianakis, G.M., Olson, J.J., Mikkelsen, T., Lehman, N., Aldape, K., *et al.* (2008) Comprehensive genomic characterization defines human glioblastoma genes and core pathways. *Nature*, **455**(7216): 1061–1068.

Miles, D.W. (2001) Update on HER-2 as a target for cancer therapy: herceptin in the clinical setting. *Breast Cancer Res*, **3**(6): 380–384.

Mortazavi, A., Williams, B.A., McCue, K., Schaeffer, L., and Wold, B. (2008) Mapping and quantifying mammalian transcriptomes by RNA-Seq. *Nat Methods*, **5**(7): 621–628.

Muzny, D.M., Bainbridge, M.N., Chang, K., Dinh, H.H., Drummond, J.A., Fowler, G., Kovar, C.L., Lewis, L.R., Morgan, M.B., Newsham, I.F., *et al.* (2012) Comprehensive molecular characterization of human colon and rectal cancer. *Nature*, **487**(7407): 330–337.

Nagalla, S., Chou, J.W., Willingham, M.C., Ruiz, J., Vaughn, J.P., Dubey, P., Lash, T.L., Hamilton-Dutoit, S.J., Bergh, J., Sotiriou, C., *et al.* (2013) Interactions between immunity, proliferation and molecular subtype in breast cancer prognosis. *Genome Biol*, **14**(4): R34.

Neeley, E.S., Kornblau, S.M., Coombes, K.R., and Baggerly, K.A. (2009) Variable slope normalization of reverse phase protein arrays. *Bioinformatics*, **25**(11): 1384.

Novomestky, F. (2012) *matrixcalc: Collection of functions for matrix calculations.* R package version 1.0-3.

Oliveira, C., Senz, J., Kaurah, P., Pinheiro, H., Sanges, R., Haegert, A., Corso, G., Schouten, J., Fitzgerald, R., Vogelsang, H., *et al.* (2009) Germline *CDH1* deletions in hereditary diffuse gastric cancer families. *Human Molecular Genetics*, **18**(9): 1545–1555.

Oliveira, C., Seruca, R., Hoogerbrugge, N., Ligtenberg, M., and Carneiro, F. (2013) Clinical utility gene card for: Hereditary diffuse gastric cancer (HDGC). *Eur J Hum Genet*, **21**(8).

Pandey, G., Zhang, B., Chang, A.N., Myers, C.L., Zhu, J., Kumar, V., and Schadt, E.E. (2010) An integrative multi-network and multi-classifier approach to predict genetic interactions. *PLoS Comput Biol*, **6**(9).

Parker, J., Mullins, M., Cheung, M., Leung, S., Voduc, D., Vickery, T., Davies, S., Fauron, C., He, X., Hu, Z., *et al.* (2009) Supervised risk predictor of breast cancer based on intrinsic subtypes. *Journal of Clinical Oncology*, **27**(8): 1160–1167.

Pereira, B., Chin, S.F., Rueda, O.M., Vollan, H.K., Provenzano, E., Bardwell, H.A., Pugh, M., Jones, L., Russell, R., Sammut, S.J., *et al.* (2016) Erratum: The somatic mutation profiles of 2,433 breast cancers refine their genomic and transcriptomic landscapes. *Nat Commun*, **7**: 11908.

Perou, C.M., Sørlie, T., Eisen, M.B., van de Rijn, M., Jeffrey, S.S., Rees, C.A., Pollack, J.R., Ross, D.T., Johnsen, H., Akslen, L.A., *et al.* (2000) Molecular portraits of human breast tumours. *Nature*, **406**(6797): 747–752.

Polyak, K. and Weinberg, R.A. (2009) Transitions between epithelial and mesenchymal states: acquisition of malignant and stem cell traits. *Nat Rev Cancer*, **9**(4): 265–73.

Prahallad, A., Sun, C., Huang, S., Di Nicolantonio, F., Salazar, R., Zecchin, D., Beijersbergen, R.L., Bardelli, A., and Bernards, R. (2012) Unresponsiveness of colon cancer to *BRAF*(v600e) inhibition through feedback activation of egfr. *Nature*, **483**(7387): 100–3.

R Core Team (2016) *R: A Language and Environment for Statistical Computing*. R Foundation for Statistical Computing, Vienna, Austria. R version 3.3.2.

Ravnan, M.C. and Matalka, M.S. (2012) Vemurafenib in patients with *BRAF* v600e mutation-positive advanced melanoma. *Clin Ther*, **34**(7): 1474–86.

Ritchie, M.E., Phipson, B., Wu, D., Hu, Y., Law, C.W., Shi, W., and Smyth, G.K. (2015) limma powers differential expression analyses for RNA-sequencing and microarray studies. *Nucleic Acids Research*, **43**(7): e47.

Robinson, M.D. and Oshlack, A. (2010) A scaling normalization method for differential expression analysis of RNA-seq data. *Genome Biol*, **11**(3): R25.

Roguev, A., Bandyopadhyay, S., Zofall, M., Zhang, K., Fischer, T., Collins, S.R., Qu, H., Shales, M., Park, H.O., Hayles, J., *et al.* (2008) Conservation and rewiring of functional modules revealed by an epistasis map in fission yeast. *Science*, **322**(5900): 405–10.

Roychowdhury, S. and Chinnaiyan, A.M. (2016) Translating cancer genomes and transcriptomes for precision oncology. *CA Cancer J Clin*, **66**(1): 75–88.

Rung, J. and Brazma, A. (2013) Reuse of public genome-wide gene expression data. *Nat Rev Genet*, **14**(2): 89–99.

Rustici, G., Kolesnikov, N., Brandizi, M., Burdett, T., Dylag, M., Emam, I., Farne, A., Hastings, E., Ison, J., Keays, M., *et al.* (2013) ArrayExpress update–trends in database growth and links to data analysis tools. *Nucleic Acids Res*, **41**(Database issue): D987–990.

Ryan, C., Lord, C., and Ashworth, A. (2014) Daisy: Picking synthetic lethals from cancer genomes. *Cancer Cell*, **26**(3): 306–308.

Schena, M. (1996) Genome analysis with gene expression microarrays. *Bioessays*, **18**(5): 427–431.

Scheuer, L., Kauff, N., Robson, M., Kelly, B., Barakat, R., Satagopan, J., Ellis, N., Hensley, M., Boyd, J., Borgen, P., *et al.* (2002) Outcome of preventive surgery and screening for breast and ovarian cancer in BRCA mutation carriers. *J Clin Oncol*, **20**(5): 1260–1268.

Semb, H. and Christofori, G. (1998) The tumor-suppressor function of E-cadherin. *Am J Hum Genet*, **63**(6): 1588–93.

Sing, T., Sander, O., Beerenwinkel, N., and Lengauer, T. (2005) Rocr: visualizing classifier performance in r. *Bioinformatics*, **21**(20): 7881.

Slurm development team (Slurm) (2017) Slurm workload manager. `https://slurm.schedmd.com/`. Accessed: 25/03/2017.

Sørlie, T., Perou, C.M., Tibshirani, R., Aas, T., Geisler, S., Johnsen, H., Hastie, T., Eisen, M.B., van de Rijn, M., Jeffrey, S.S., *et al.* (2001) Gene expression patterns of breast carcinomas distinguish tumor subclasses with clinical implications. *Proc Natl Acad Sci USA*, **98**(19): 10869–10874.

Stajich, J.E. and Lapp, H. (2006) Open source tools and toolkits for bioinformatics: significance, and where are we? *Brief Bioinformatics*, **7**(3): 287–296.

Stratton, M.R., Campbell, P.J., and Futreal, P.A. (2009) The cancer genome. *Nature*, **458**(7239): 719–724.

Ström, C. and Helleday, T. (2012) Strategies for the use of poly(adenosine diphosphate ribose) polymerase (parp) inhibitors in cancer therapy. *Biomolecules*, **2**(4): 635–649.

Sun, C., Wang, L., Huang, S., Heynen, G.J.J.E., Prahallad, A., Robert, C., Haanen, J., Blank, C., Wesseling, J., Willems, S.M., *et al.* (2014) Reversible and adaptive resistance to *BRAF*(v600e) inhibition in melanoma. *Nature*, **508**(7494): 118–122.

Telford, B.J., Chen, A., Beetham, H., Frick, J., Brew, T.P., Gould, C.M., Single, A., Godwin, T., Simpson, K.J., and Guilford, P. (2015) Synthetic lethal screens identify vulnerabilities in gpcr signalling and cytoskeletal organization in E-cadherin-deficient cells. *Mol Cancer Ther*, **14**(5): 1213–1223.

The 1000 Genomes Project Consortium (1000 Genomes) (2010) A map of human genome variation from population-scale sequencing. *Nature*, **467**(7319): 1061–1073.

The Cancer Genome Atlas Research Network (TCGA) (2012) Comprehensive molecular portraits of human breast tumours. *Nature*, **490**(7418): 61–70.

The Cancer Genome Atlas Research Network (TCGA) (2017) The Cancer Genome Atlas Project. `https://cancergenome.nih.gov/`. Accessed: 26/03/2017.

The Catalogue Of Somatic Mutations In Cancer (COSMIC) (2016) Cosmic: The catalogue of somatic mutations in cancer. `http://cancer.sanger.ac.uk/cosmic`. Release 79 (23/08/2016), Accessed: 05/02/2017.

The Comprehensive R Archive Network (CRAN) (2017) Cran. `https://cran.r-project.org/`. Accessed: 24/03/2017.

The ENCODE Project Consortium (ENCODE) (2004) The ENCODE (ENCyclopedia Of DNA Elements) Project. *Science*, **306**(5696): 636–640.

The National Cancer Institute (NCI) (2015) The genetics of cancer. `https://www.cancer.gov/about-cancer/causes-prevention/genetics`. Published: 22/04/2015, Accessed: 22/03/2017.

The New Zealand eScience Infrastructure (NeSI) (2017) NeSI. `https://www.nesi.org.nz/`. Accessed: 25/03/2017.

The Pharmaceutical Management Agency (PHARMAC) (2012) Ucsc cancer genomics browser. Accessed 29th March 2012.

Tierney, L., Rossini, A.J., Li, N., and Sevcikova, H. (2015) *snow: Simple Network of Workstations*. R package version 0.4-2.

Tiong, K.L., Chang, K.C., Yeh, K.T., Liu, T.Y., Wu, J.H., Hsieh, P.H., Lin, S.H., Lai, W.Y., Hsu, Y.C., Chen, J.Y., *et al.* (2014) Csnk1e/ctnnb1 are synthetic lethal to tp53 in colorectal cancer and are markers for prognosis. *Neoplasia*, **16**(5): 441–50.

Tischler, J., Lehner, B., and Fraser, A.G. (2008) Evolutionary plasticity of genetic interaction networks. *Nat Genet*, **40**(4): 390–391.

Tomasetti, C. and Vogelstein, B. (2015) Cancer etiology. Variation in cancer risk among tissues can be explained by the number of stem cell divisions. *Science*, **347**(6217): 78–81.

Tong, A.H., Evangelista, M., Parsons, A.B., Xu, H., Bader, G.D., Page, N., Robinson, M., Raghibizadeh, S., Hogue, C.W., Bussey, H., *et al.* (2001) Systematic genetic analysis with ordered arrays of yeast deletion mutants. *Science*, **294**(5550): 2364–8.

Tong, A.H., Lesage, G., Bader, G.D., Ding, H., Xu, H., Xin, X., Young, J., Berriz, G.F., Brost, R.L., Chang, M., *et al.* (2004) Global mapping of the yeast genetic interaction network. *Science*, **303**(5659): 808–13.

Tran, B., Dancey, J.E., Kamel-Reid, S., McPherson, J.D., Bedard, P.L., Brown, A.M., Zhang, T., Shaw, P., Onetto, N., Stein, L., *et al.* (2012) Cancer genomics: technology, discovery, and translation. *J Clin Oncol*, **30**(6): 647–660.

Travers, J. and Milgram, S. (1969) An experimental study of the small world problem. *Sociometry*, **32**(4): 425–443.

Tsai, H.C., Li, H., Van Neste, L., Cai, Y., Robert, C., Rassool, F.V., Shin, J.J., Harbom, K.M., Beaty, R., Pappou, E., *et al.* (2012) Transient low doses of dna-demethylating agents exert durable antitumor effects on hematological and epithelial tumor cells. *Cancer Cell*, **21**(3): 430–46.

Tunggal, J.A., Helfrich, I., Schmitz, A., Schwarz, H., Gunzel, D., Fromm, M., Kemler, R., Krieg, T., and Niessen, C.M. (2005) E-cadherin is essential for in vivo epidermal barrier function by regulating tight junctions. *EMBO J*, **24**(6): 1146–1156.

Tutt, A., Robson, M., Garber, J.E., Domchek, S.M., Audeh, M.W., Weitzel, J.N., Friedlander, M., Arun, B., Loman, N., Schmutzler, R.K., *et al.* (2010) Oral poly(adp-ribose) polymerase inhibitor olaparib in patients with *BRCA1* or *BRCA2* mutations and advanced breast cancer: a proof-of-concept trial. *Lancet*, **376**(9737): 235–44.

van der Meer, R., Song, H.Y., Park, S.H., Abdulkadir, S.A., and Roh, M. (2014) RNAi screen identifies a synthetic lethal interaction between PIM1 overexpression and PLK1 inhibition. *Clinical Cancer Research*, **20**(12): 3211–3221.

van der Post, R.S., Vogelaar, I.P., Carneiro, F., Guilford, P., Huntsman, D., Hoogerbrugge, N., Caldas, C., Schreiber, K.E., Hardwick, R.H., Ausems, M.G., *et al.* (2015) Hereditary diffuse gastric cancer: updated clinical guidelines with an emphasis on germline CDH1 mutation carriers. *J Med Genet*, **52**(6): 361–374.

van Steen, K. (2012) Travelling the world of genegene interactions. *Briefings in Bioinformatics*, **13**(1): 1–19.

van Steen, M. (2010) *Graph Theory and Complex Networks: An Introduction*. Maarten van Steen, VU Amsterdam.

Vapnik, V.N. (1995) *The nature of statistical learning theory*. Springer-Verlag New York, Inc.

Vizeacoumar, F.J., Arnold, R., Vizeacoumar, F.S., Chandrashekhar, M., Buzina, A., Young, J.T., Kwan, J.H., Sayad, A., Mero, P., Lawo, S., *et al.* (2013) A negative genetic interaction map in isogenic cancer cell lines reveals cancer cell vulnerabilities. *Mol Syst Biol*, **9**: 696.

Vogelstein, B., Papadopoulos, N., Velculescu, V.E., Zhou, S., Diaz, L.A., and Kinzler, K.W. (2013) Cancer genome landscapes. *Science*, **339**(6127): 1546–1558.

Vos, C.B., Cleton-Jansen, A.M., Berx, G., de Leeuw, W.J., ter Haar, N.T., van Roy, F., Cornelisse, C.J., Peterse, J.L., and van de Vijver, M.J. (1997) E-cadherin inactivation in lobular carcinoma in situ of the breast: an early event in tumorigenesis. *Br J Cancer*, **76**(9): 1131–3.

Waldron, D. (2016) Cancer genomics: A multi-layer omics approach to cancer. *Nat Rev Genet*, **17**(8): 436–437.

Wang, K., Singh, D., Zeng, Z., Coleman, S.J., Huang, Y., Savich, G.L., He, X., Mieczkowski, P., Grimm, S.A., Perou, C.M., *et al.* (2010) MapSplice: accurate mapping of RNA-seq reads for splice junction discovery. *Nucleic Acids Res*, **38**(18): e178.

Wang, X. and Simon, R. (2013) Identification of potential synthetic lethal genes to p53 using a computational biology approach. *BMC Medical Genomics*, **6**(1): 30.

Wappett, M. (2014) Bisep: Toolkit to identify candidate synthetic lethality. r package version 2.0.

Wappett, M., Dulak, A., Yang, Z.R., Al-Watban, A., Bradford, J.R., and Dry, J.R. (2016) Multi-omic measurement of mutually exclusive loss-of-function enriches for candidate synthetic lethal gene pairs. *BMC Genomics*, **17**: 65.

Warnes, G.R., Bolker, B., Bonebakker, L., Gentleman, R., Liaw, W.H.A., Lumley, T., Maechler, M., Magnusson, A., Moeller, S., Schwartz, M., *et al.* (2015) *gplots: Various R Programming Tools for Plotting Data*. R package version 2.17.0.

Watts, D.J. and Strogatz, S.H. (1998) Collective dynamics of 'small-world' networks. *Nature*, **393**(6684): 440–2.

Weinstein, I.B. (2000) Disorders in cell circuitry during multistage carcinogenesis: the role of homeostasis. *Carcinogenesis*, **21**(5): 857–864.

Weinstein, J.N., Collisson, E.A., Mills, G.B., Shaw, K.R., Ozenberger, B.A., Ellrott, K., Shmulevich, I., Sander, C., Stuart, J.M., Chang, K., *et al.* (2013) The Cancer Genome Atlas Pan-Cancer analysis project. *Nat Genet*, **45**(10): 1113–1120.

Wickham, H. and Chang, W. (2016) *devtools: Tools to Make Developing R Packages Easier*. R package version 1.12.0.

Wickham, H., Danenberg, P., and Eugster, M. (2017) *roxygen2: In-Line Documentation for R*. R package version 6.0.1.

Wong, S.L., Zhang, L.V., Tong, A.H.Y., Li, Z., Goldberg, D.S., King, O.D., Lesage, G., Vidal, M., Andrews, B., Bussey, H., *et al.* (2004) Combining biological networks to predict genetic interactions. *Proceedings of the National Academy of Sciences of the United States of America*, **101**(44): 15682–15687.

World Health Organization (WHO) (2017) Fact sheet: Cancer. `http://www.who.int/mediacentre/factsheets/fs297/en/`. Updated February 2017, Accessed: 22/03/2017.

Wu, M., Li, X., Zhang, F., Li, X., Kwoh, C.K., and Zheng, J. (2014) In silico prediction of synthetic lethality by meta-analysis of genetic interactions, functions, and pathways in yeast and human cancer. *Cancer Inform*, **13**(Suppl 3): 71–80.

Yu, H. (2002) Rmpi: Parallel statistical computing in r. *R News*, **2**(2): 10–14.

Zhang, F., Wu, M., Li, X.J., Li, X.L., Kwoh, C.K., and Zheng, J. (2015) Predicting essential genes and synthetic lethality via influence propagation in signaling pathways of cancer cell fates. *J Bioinform Comput Biol*, **13**(3): 1541002.

Zhang, J., Baran, J., Cros, A., Guberman, J.M., Haider, S., Hsu, J., Liang, Y., Rivkin, E., Wang, J., Whitty, B., *et al.* (2011) International cancer genome consortium data portala one-stop shop for cancer genomics data. *Database: The Journal of Biological Databases and Curation*, **2011**: bar026.

Zhong, W. and Sternberg, P.W. (2006) Genome-wide prediction of c. elegans genetic interactions. *Science*, **311**(5766): 1481–1484.

Zweig, M.H. and Campbell, G. (1993) Receiver-operating characteristic (roc) plots: a fundamental evaluation tool in clinical medicine. *Clinical Chemistry*, **39**(4): 561–577.